On the resonance eigenstates of an open quantum baker map

2008 Nonlinearity 21 2591

(http://iopscience.iop.org/0951-7715/21/11/007)

Nonlinearity **21** (2008) 2591–2624 doi:10.1088/0951-7715/21/11/007

On the resonance eigenstates of an open quantum baker map

J P Keating[1], S Nonnenmacher[2,3], M Novaes[1] and M Sieber[1]

[1] School of Mathematics, University of Bristol, Bristol BS8 1TW, UK
[2] Institut de Physique Théorique, CEA, IPhT, F-91191 Gif-sur-Yvette, France
[3] CNRS, URA 2306, F-91191 Gif-sur-Yvette, France

Received 4 June 2008, in final form 29 August 2008
Published 29 September 2008
Online at stacks.iop.org/Non/21/2591

Recommended by B Eckhardt

Abstract
We study the resonance eigenstates of a particular quantization of the open baker map. For any admissible value of Planck's constant, the corresponding quantum map is a subunitary matrix, and the nonzero component of its spectrum is contained inside an annulus in the complex plane, $|z_{\min}| \leqslant |z| \leqslant |z_{\max}|$. We consider semiclassical sequences of eigenstates, such that the moduli of their eigenvalues converge to a fixed radius r. We prove that if the moduli converge to $r = |z_{\max}|$ then the sequence of eigenstates is associated with a fixed phase space measure $\rho_{\max}$. The same holds for sequences with eigenvalue moduli converging to $|z_{\min}|$, with a different limit measure $\rho_{\min}$. Both these limiting measures are supported on fractal sets, which are trapped sets of the classical dynamics. For a general radius $|z_{\min}| < r < |z_{\max}|$ there is no unique limit measure, and we identify some families of eigenstates with precise self-similar properties.

Mathematics Subject Classification: 35B34, 37D20, 81Q50, 81U15

1. Introduction

In the semiclassical limit, stationary states of quantum systems are in general expected to concentrate on phase space structures that are invariant under the corresponding classical dynamics [6, 43]. More precisely, any semiclassical sequence of eigenstates of energies $\sim E$ is associated with one or several semiclassical limit measures, which are probability measures on the energy shell Σ_E, invariant under the Hamiltonian flow. We will say that the semiclassical sequence of eigenstates converges to one or several limit measures.

According to the quantum ergodicity theorem [11, 20, 40, 44], if the classical flow on some energy shell Σ_E is ergodic with respect to the Liouville measure, then in the semiclassical limit almost all quantum eigenstates of energy $\sim E$ become (in a weak sense) equidistributed on the energy shell; for a recent review, see for instance [45]. This means that almost all such semiclassical sequences converge to the Liouville measure on Σ_E.

Canonical maps on the two-dimensional torus, such as the baker map [2, 19, 36], the cat map [18, 21] and their generalizations [22], can be quantized to give finite-dimensional unitary matrices. Such quantum maps have been widely used as toy models in the context of quantum chaos, because they possess several simplifying properties: two-dimensional torus phase space instead of Σ_E, simple symbolic dynamics, finite-dimensional quantum mechanics, easy numerical implementation (see, for example, [13]). If the map is ergodic with respect to the Liouville (= Lebesgue) measure, then a quantum ergodicity theorem states that almost all sequences of eigenstates of the quantized map become uniformly distributed on the torus in the semiclassical limit [7, 12, 26, 25]. (Quantum ergodicity has also recently been established for certain families of quantum graphs [3], but for other families it is known not to hold [4, 5].)

It is important to remark that, in general, a chaotic system admits many invariant measures different from the Liouville measure, e.g. delta measures carried on periodic orbits, or fractal measures. Even when the system is quantum ergodic, exceptional sequences of eigenstates could converge to some of these invariant measures. Such exceptional eigenstates have been constructed for several types of quantized ergodic maps on the torus [1, 9, 16]. On the other hand, ergodic systems for which all sequences of eigenstates converge to the Liouville measure are said to obey quantum unique ergodicity (QUE). This is obviously the case when there exist no invariant measures other than the Liouville measure [30, 34]. Some ergodic systems carry arithmetic structures (typically, a commuting family of 'Hecke' operators commuting with the quantum dynamics), which lead one to consider joint ('Hecke') eigenstates. In that case, one can sometimes prove that all the Hecke eigenstates semiclassically converge to the Liouville measure, a property called arithmetic quantum unique ergodicity [24, 28, 35].

The corresponding properties of open (scattering) chaotic systems are currently not nearly as well understood. The invariant properties of the classical open system are related to the set of trapped trajectories, called the trapped set. For a chaotic system, this trapped set is generally a *fractal repeller*. The statistical properties of the system can be associated with conditionally invariant measures, or eigenmeasures of the propagator, which are only invariant up to a constant (the decay rate of the measure). A recent review of the theory of classical chaotic systems with openings can be found in [14]. In the quantum version of the problem each resonant state has a specific decay rate. For the system studied here we show that a form of QUE holds for *extremal* decay rates, whilst multiple limit measures exist in the bulk. Because the notion of ergodicity is not clearly defined for the open system, it would be more correct to use the phrase 'quantum uniqueness' rather than QUE, but the latter has the advantage of connecting us with previous works on closed chaotic systems.

1.1. Open chaotic maps

Instead of dealing with a genuine scattering system (with infinite-volume phase space), it is simpler to consider a discrete-time dynamical system (that is, a map) living on a compact phase space, but with a 'hole' through which the particles escape, never to return (the map is then said to be 'open'). This compact phase space is a model for the 'interaction region' of a realistic scattering system. Open maps may also be quantized, into subunitary matrices (see below). One expects the spectrum of these quantum maps to (at least qualitatively) mimic the properties of the resonances and the resonant states of scattering systems.

We focus here on a specific quantization of the open baker map, for which we prove some conjectures pertaining to the semiclassical behaviour of (resonant) eigenstates [23, 31].

Before stating our results, we describe the general construction of an open map on the torus.

Consider an invertible canonical map $\mathcal{U}$ on the two-dimensional torus T (viewed as a phase space). We assume that $\mathcal{U}$ is chaotic, in particular that it is ergodic with respect to the Liouville measure on T. Let this map be 'opened' by identifying some region of phase space with a 'hole' through which points escape, and denote the resulting open map by $\tilde{\mathcal{U}}$. The ergodicity of $\mathcal{U}$ implies that almost all initial conditions escape the system when propagated either forwards or backwards. The set of initial conditions that remain trapped for infinite times when propagated to the future (respectively the past) is called the forward-trapped (respectively backward-trapped) set and denoted by K_- (respectively K_+).

All invariant measures are supported on the intersection $K_0 = K_+ \cap K_-$, which is the trapped set or the repeller. The sets K_- and K_+ are the stable and unstable manifolds of the repeller, respectively. We denote the opening by O, and by $O_m = \mathcal{U}^m(O)$ its image under the mth power of the closed map. The trapped sets are then defined as

$$K_- = T \setminus \bigcup_{m=0}^{\infty} O_{-m}, \qquad K_+ = T \setminus \bigcup_{m=1}^{\infty} O_m. \tag{1}$$

1.2. Open quantum maps

We choose to quantize the torus using *antiperiodic* boundary conditions for the wavefunctions, so that both position and momentum take values of the form (integer + $1/2)/N$ [18]. In the position representation, quantum states are thus given by a 'comb' of delta functions supported on the set

$$S_N = \left\{ q_j = \frac{j+1/2}{N}, 0 \leqslant j \leqslant N-1 \right\}. \tag{2}$$

These quantum states form a Hilbert space of dimension N, where N plays the role of an effective Planck's constant, $\hbar = (2\pi N)^{-1}$. The quantization of the invertible canonical map $\mathcal{U}$ is a unitary matrix U acting on this Hilbert space. Its eigenvalues therefore lie on the unit circle.

We shall open our map by taking the hole to be a strip parallel to the momentum axis, of the form $O = I \times [0, 1)$. At the quantum level, we call Π the projector on the subspace spanned by the positions in $q_j \in I$. The complementary projector $(1 - \Pi)$ kills (at each step of the dynamics) the states localized in the hole, and lets the others evolve through the propagator U. Hence, the quantum version of the open map is given by the (nonunitary) matrix $\tilde{U} = U(1 - \Pi)$. The result of multiplying by $1 - \Pi$ is to set to zero the columns of U corresponding to the hole. The matrix $\tilde{U}$ is not normal, so we must distinguish between its right and left eigenstates,

$$\tilde{U}|\Psi_n^{\mathrm{R}}\rangle = z_n|\Psi_n^{\mathrm{R}}\rangle, \qquad \langle\Psi_n^{\mathrm{L}}|\tilde{U} = z_n\langle\Psi_n^{\mathrm{L}}|. \tag{3}$$

We shall assume the eigenstates to be normalized according to $\langle\Psi_n^{\mathrm{L}}|\Psi_n^{\mathrm{L}}\rangle = \langle\Psi_n^{\mathrm{R}}|\Psi_n^{\mathrm{R}}\rangle = 1$, instead of the usual $\langle\Psi_n^{\mathrm{L}}|\Psi_m^{\mathrm{R}}\rangle = \delta_{nm}$. The eigenvalues z_n of $\tilde{U}$ lie in the unit disc, $|z_n|^2 = \mathrm{e}^{-\Gamma_n} \leqslant 1$; $\Gamma_n \geqslant 0$ is called the decay rate associated with the eigenstate $|\Psi_n^{\mathrm{R}}\rangle$.

The usual Weyl law for closed systems relates (in the semiclassical limit) the mean eigenvalue density to the available phase space volume. For open chaotic systems the mean density of resonances is believed to be determined by the fractal dimension of the repeller, a property known as the fractal Weyl law [29]. This law was investigated numerically for two-dimensional Hamiltonian scattering systems [17, 27, 29], for the baker map [32, 33] and for the kicked rotator [39]. It has been proven for the Walsh-baker map [32, 33] (see below). Although a fractal upper bound on the number of resonances has been proven for Hamiltonian scattering systems [41], the fractal Weyl law still stands as a conjecture for generic open systems. In [39] a heuristic argument for this law was presented, based on the distinction between *short-lived* and *long-lived* eigenstates. The short-lived states are associated with phase space regions that escape in a short time (comparable to the Ehrenfest time), so that their decay rate satisfies $\Gamma_n \gg 1$. On the other hand, long-lived states remain in the system long enough to develop strong diffraction and interference effects, leading to a finite decay rate $\Gamma_n = \mathcal{O}(1)$. The latter will be the main focus of our investigation.

1.3. Semiclassical limit of 'resonant' eigenstates

To further motivate this work, we summarize here some recent heuristic arguments and numerical results. Eigenstates of open chaotic maps were studied in a general setting by Keating *et al* in [23]. They were represented in phase space by using Husimi functions

$$H_\psi(x) = \frac{1}{2\pi\hbar}|\langle x|\psi\rangle|^2, \tag{4}$$

where x is a point in phase space and $|x\rangle$ a standard Gaussian coherent state. It was shown that, in the semiclassical limit, the phase space support of long-lived right (respectively left) eigenstates must be a subset of the backward (respectively forward) trapped set, in the sense that

$$\lim_{\hbar\to 0} H_{\Psi_n^{\mathrm{R}}}(x) = 0 \quad \text{if } x \notin K_+, \qquad \text{respectively} \qquad \lim_{\hbar\to 0} H_{\Psi_n^{L}}(x) = 0 \quad \text{if } x \notin K_-. \tag{5}$$

For maps on the torus it was shown that if $\Pi_1 = \Pi$ is the projector onto the opening and Π_{m+1} the projector onto the set of points which reach the opening after m steps but not earlier, then within the semiclassical approximation one has $\Pi_{m+1} \approx (\tilde{U}^\dagger)^m \Pi_1 \tilde{U}^m$ and therefore

$$\langle \Psi_n^{\mathrm{R}}|\Pi_{m+1}|\Psi_n^{\mathrm{R}}\rangle \approx |z_n|^{2m}(1-|z_n|^2). \tag{6}$$

The specific system studied numerically in [23] was the triadic baker map, defined by

$$\mathcal{U}(q,p) = \begin{cases} \left(3q, \dfrac{p}{3}\right) & \text{if } 0 \leqslant q < \dfrac{1}{3}, \\ \left(3q-1, \dfrac{p+1}{3}\right) & \text{if } \dfrac{1}{3} \leqslant q < \dfrac{2}{3}, \\ \left(3q-2, \dfrac{p+2}{3}\right) & \text{if } \dfrac{2}{3} \leqslant q < 1. \end{cases} \tag{7}$$

This map was opened by sending 'to infinity' points in the middle vertical strip; in this case, K_- is the product Can $\times$ [0, 1), where Can denotes the usual middle-third Cantor set, and $K_+ = [0,1) \times$ Can. The closed baker map was quantized in [2, 19, 36]. Taking the opening into account, one obtains the matrix [37]

$$\tilde{U} = F_N^\dagger \begin{pmatrix} F_{N/3} & & \\ & 0 & \\ & & F_{N/3} \end{pmatrix}. \tag{8}$$

Here F_N is the discrete Fourier transform on the set S_N,

$$(F_N)_{nm} = \frac{1}{\sqrt{N}} \mathrm{e}^{-\frac{2\pi\mathrm{i}}{N}(n+1/2)(m+1/2)}, \qquad n, m \in \{0, \ldots, N-1\}. \tag{9}$$

The numerical computations in [23] were restricted to values of $N = (2\pi\hbar)^{-1}$ given by $N = 3^k$, such that the semiclassical limit corresponds to $k \to \infty$. In figure 1 we plot the

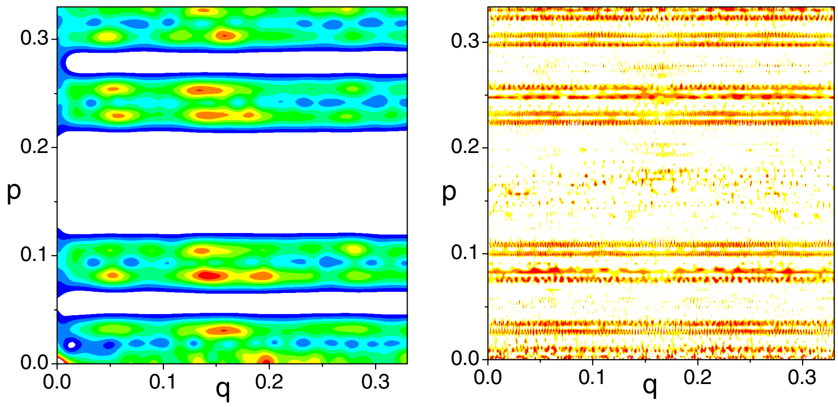

Figure 1. Left panel: the average of the Husimi functions (4) of the 100 longest-lived right eigenstates of the baker map, for $N = 3^7$ (intensity increases from blue to red). Right panel: the corresponding Wigner function average (in the white regions the function is nonpositive). Taken from [23].

(This figure is in colour only in the electronic version)

Husimi function of right eigenstates, averaged over the 100 longest-living states, for the case $N = 3^7$. This function is approximately concentrated on the backward-trapped set. The right panel shows the averaged Wigner function [18], which resolves K_+ with higher accuracy.

Nonnenmacher and Rubin considered eigenstates of the open quantum baker (8) in [31] (in their case, F_N is the discrete Fourier transform on the set $\{j/N,\ j = 0, \ldots, N-1\}$). They showed, in particular, that if a point x is at a finite distance from K_+ and from the set of discontinuities of the classical map $\mathcal{U}$, then in the semiclassical limit the property (5) is a consequence of the stronger estimate

$$H_{\Psi_n^{\mathrm{R}}}(x) = \mathcal{O}(\mathrm{e}^{-cN}), \qquad N \to \infty. \tag{10}$$

They also showed that for any semiclassical sequence of (right) eigenstates $(\Psi_N)_{N\to\infty}$ such that $\lim_{N\to\infty} |z_N|^2 = \mathrm{e}^{-\Gamma}$, the Husimi measures H_{Ψ_N} weak-$*$ converge to one or several probability measures on the torus: each of these limit measures is necessarily an *eigenmeasure* (also called conditionally invariant measure) of the open map $\tilde{\mathcal{U}}$, with the eigenvalue $\mathrm{e}^{-\Gamma}$. The semiclassical estimate (6) is then a consequence of the conditional invariance of limit measures.

1.4. The Walsh-baker map

When $N = 3^k$, an alternative quantization of the baker map (7) exists, which is based on a modified Fourier transform, the Walsh–Fourier transform [32, 33]. The Walsh-baker map can be solved exactly, with explicit expressions for the spectrum and the eigenstates. Its open version is the only system for which a fractal Weyl law has been rigorously proven. In the Walsh framework, the phase space distribution of eigenstates can be studied through a Walsh version of the Husimi measure, called the Walsh–Husimi measure (see section 2.4). This measure is defined on 'quantum rectangles' (also called 'tiles' [42]).

Let us recall the definition of a 'rectangle' in phase space. Let us denote by

$$q - \frac{1}{2N} = 0 \cdot \epsilon_1\epsilon_2\epsilon_3 \cdots \tag{11}$$

the number $q - \frac{1}{2N} \in [0, 1)$, the ternary decomposition of which is given by

$$q - \frac{1}{2N} = \sum_{\ell=1}^{\infty} \epsilon_\ell \, 3^{-\ell}, \qquad \epsilon_\ell \in \{0, 1, 2\}. \tag{12}$$

For any $b \in \mathbb{N}$, a sequence $\boldsymbol{\epsilon} = \epsilon_1 \cdots \epsilon_b$ describes an interval of length 3^{-b} in the position axis, which we denote by $[\boldsymbol{\epsilon}]$. If, for some $b' \in \mathbb{N}$, $[\boldsymbol{\epsilon}' = \epsilon'_1 \cdots \epsilon'_{b'}]$ describes a similar triadic interval in the momentum axis, then the product of these two intervals, which is a rectangle of area $3^{-b-b'}$, will be denoted by $[\epsilon'_{b'} \cdots \epsilon'_1 \cdot \epsilon_1 \cdots \epsilon_b]$ (notice the inversion of indices for $\boldsymbol{\epsilon}'$).

In the following, we will often refer to the case where $b = b' = v$, for some fixed $v > 0$, which we will call a *v-square* and denote it by $[\boldsymbol{\epsilon}' \cdot \boldsymbol{\epsilon}]_v$. A rectangle of size $v \times 0$ will be called *vertical*, and denoted by $[\cdot \boldsymbol{\epsilon}]_v$. If on the other hand b, b' are related by $b' = k - b$ (where k is the quantum parameter), then $[\boldsymbol{\epsilon}' \cdot \boldsymbol{\epsilon}]$ will be called a 'quantum rectangle'. For each $b \in [0, k]$, the Walsh–Husimi measure H^b_Ψ is defined by its weights on the rectangles of size $b \times (k-b)$, denoted by $H^b_\Psi([\boldsymbol{\epsilon}' \cdot \boldsymbol{\epsilon}])$. One recovers the position (respectively Walsh-momentum) representation by taking $b = k$ (respectively $b = 0$):

$$H^k_\Psi([\cdot \boldsymbol{\epsilon}]) = |\langle q|\Psi\rangle|^2 \qquad \text{for } q = 0.\epsilon_1 \cdots \epsilon_k + \frac{1}{2N}, \tag{13}$$

$$H^0_\Psi([\boldsymbol{\epsilon}' \cdot]) = |\langle p|\Psi\rangle|^2 \qquad \text{for } p = 0.\epsilon'_1 \cdots \epsilon'_k + \frac{1}{2N}. \tag{14}$$

We will need to compute the value of a Walsh–Husimi measure on 'classical' v-squares $[\boldsymbol{\epsilon}' \cdot \boldsymbol{\epsilon}]_v$, for which v is independent of k. We define this in the natural way, taking $H^b_\Psi([\boldsymbol{\epsilon}' \cdot \boldsymbol{\epsilon}]_v)$ to be the sum of the values of H^b_Ψ over all quantum squares contained in $[\boldsymbol{\epsilon}' \cdot \boldsymbol{\epsilon}]_v$ (see (43)).

The Walsh quantization of the *closed* baker map was studied in [1]: the authors proved quantum ergodicity but found several counterexamples to QUE. In particular, they constructed semiclassical sequences of eigenstates along which the Walsh–Husimi measures converge to (multi)fractal invariant measures.

In this work we focus on the Walsh quantization of the open baker, defined in [32, 33] and further studied in [31]. The quantum propagator is given by the following matrix ($N = 3^k$):

$$B = W_N^\dagger \begin{pmatrix} W_{N/3} & & \\ & 0 & \\ & & W_{N/3} \end{pmatrix}, \tag{15}$$

where W_N is the Walsh–Fourier transform (see (24)). The nonzero part of the spectrum forms a lattice inside the annulus $\{|z_{\min}| \leqslant |z| \leqslant |z_{\max}|\}$. We use a quantization slightly different from the one used in [31]. In our case the eigenvalues at the 'edges' of the nontrivial spectrum are given by

$$z_{\max} = 1 \qquad \text{and} \qquad z_{\min} = \frac{i}{\sqrt{3}},$$

both being nondegenerate. On the other hand, eigenvalues in the 'bulk' of the spectrum $\{|z_{\min}| < |z| < |z_{\max}|\}$ are (highly) degenerate. The kinematics of the map is such that the position representation of right eigenstates is equal to the (Walsh-)momentum representation of left eigenstates. We may therefore restrict our analysis to the study of the right eigenstates.

1.5. Statement of our results

We obtain precise results on the phase space distribution of long-living eigenstates of the open Walsh-baker map, both for finite $N = 3^k$ and in the limit $k \to \infty$. One question posed in [31] concerns the family of eigenmeasures one can obtain by taking weak-$*$ semiclassical limits of Husimi (or Walsh–Husimi) measures: for a given $\Gamma \geqslant 0$, which eigenmeasures of eigenvalue $\mathrm{e}^{-\Gamma}$ can be obtained as semiclassical limits? It was conjectured that the (right) eigenstates of B near the 'edges' of the nontrivial spectrum, i.e. such that $|z| \to |z_{\max}|$ (respectively $|z| \to |z_{\min}|$), converge to a unique measure $\rho_{\max}$ (respectively $\rho_{\min}$). In the theorem below we prove this conjecture.

An important role is played here by the Cantor set and its generations. If we denote by Can_n the set of points in the interval $[0, 1)$ such that the first n digits in their ternary decomposition are all different from 1, the sequence $(\mathrm{Can}_n)_{n\geqslant 1}$ converges to the middle-third Cantor set $\mathrm{Can} = \mathrm{Can}_\infty$. The 'uniform measure' on Can is defined as follows on triadic intervals of length n:

$$\forall \epsilon = \epsilon_1 \cdots \epsilon_n, \qquad \nu_{\mathrm{Can}}([\epsilon]) \stackrel{\mathrm{def}}{=} \begin{cases} 2^{-n} & \text{if all } \epsilon_i \in \{0, 2\}, \\ 0 & \text{otherwise.} \end{cases} \tag{16}$$

Theorem 1. *Let $(\Psi_k)_{k\to\infty}$ be a sequence of right eigenstates of the open Walsh-baker B, such that the associated eigenvalues semiclassically converge to the outer edge of the spectrum: $|z_k| \stackrel{k\to\infty}{\longrightarrow} 1$. Then the corresponding Husimi measures $(H^{[k/2]}_{\Psi_k})$ weak-$*$ converge to a unique invariant measure $\rho_{\max}$, supported on the repeller K_0. This means that $H^{[k/2]}_{\Psi_k}([\epsilon' \cdot \epsilon]_v) \stackrel{k\to\infty}{\longrightarrow} \rho_{\max}([\epsilon' \cdot \epsilon]_v)$ for any v-square $[\epsilon' \cdot \epsilon]_v$.*

Similarly, if the eigenvalues of a sequence $(\Psi_k)_{k\to\infty}$ of right eigenstates converge to the inner edge, $|z_k| \to 1/\sqrt{3}$, then the Husimi measures $H^{[k/2]}_{\Psi_k}$ converge (in the above sense) to a unique self-similar eigenmeasure $\rho_{\min}$ supported on K_+.

Both measures $\rho_{\max}$ and $\rho_{\min}$ can be factorized as $\rho = \nu_{\mathrm{Can}}(\mathrm{d}p) \times \nu_{\max/\min}(\mathrm{d}q)$, where ν_{Can} is the uniform measure (16) on the Cantor set, $\nu_{\max} = \nu_{\mathrm{Can}}$ and $\nu_{\min}$ is a certain self-similar measure on $[0, 1)$ (see (85)).

$\rho_{\max}$ is an invariant measure of the (closed) baker map $\mathcal{U}$, localized on the trapped set K_0. Loosely speaking, it is the 'uniform' measure on K_0. More precisely, it is the invariant measure of maximal entropy (and at the same time the Gibbs measure associated with the potential $-\log J^u(x)$) for the restriction of $\mathcal{U}$ to K_0 (see [10] for the description of these measures in a more general context).

Theorem 1 expresses a form of 'quantum uniqueness' at the edges of the nontrivial spectrum of B. The next theorems apply to the 'bulk' of the nontrivial spectrum and show that such a quantum uniqueness does not hold there. These theorems are concerned with a particular eigenbasis for the nontrivial spectrum (see section 3.1).

The description of this particular eigenbasis uses binary sequences $\boldsymbol{\eta} = \eta_1 \cdots \eta_k$ of length k, such that each symbol $\eta_j \in \{+, -\}$. If $\boldsymbol{\eta}$ is a periodic sequence of period ℓ, its orbit under the cyclic shift (which we denote by $[\boldsymbol{\eta}]$) consists of ℓ different sequences. We can associate with this orbit ℓ different long-lived right eigenstates of B, denoted by $\Psi^m_{\boldsymbol{\eta}}$ (see (49) in section 3.1). The respective eigenvalues are $z_{\delta,m/\ell} = z^{\delta}_{\min}\, \mathrm{e}^{2\pi \mathrm{i} m/\ell}$, where $0 \leqslant m \leqslant \ell - 1$. The number of times the symbol '+' appears in $\boldsymbol{\eta}$ is called its *degree* and is denoted by d. The variable $\delta \in [0, 1)$ is given by $\delta = d/k$ and called the *relative degree* of $\boldsymbol{\eta}$.

For any $0 \leqslant b \leqslant k$, we denote by $H^b_{\Psi^m_{\eta}}$ the Walsh–Husimi measure associated with this eigenstate. Before dealing with these individual eigenstates, it is easier to average over the phase index m, and define the averaged Husimi measure

$$H^b_{[\eta]} \stackrel{\mathrm{def}}{=} \frac{1}{\ell} \sum_{m=0}^{\ell-1} H^b_{\Psi^m_{\eta}}. \tag{17}$$

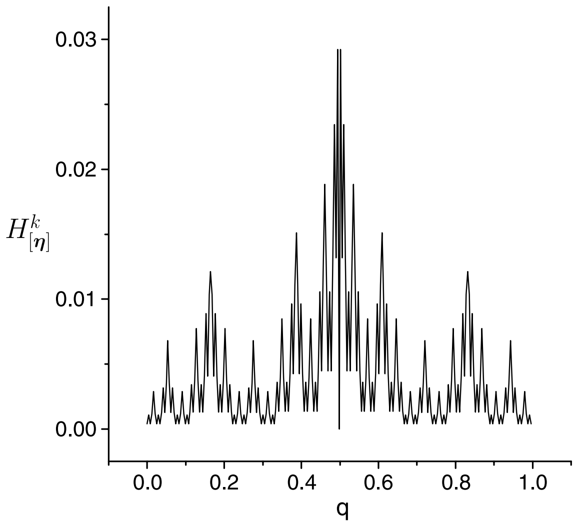

Figure 2. The position density function $H^k_{[\eta]}(q)$ for $\eta = + + + + -$.

Our understanding of these averaged measures is not only semiclassical, but already valid for finite k.

Theorem 2. *For any value of $k \geqslant 1$, any $0 \leqslant b \leqslant k$, and any sequence η of length k and degree $d = \delta k$, the averaged Walsh–Husimi measure $H^b_{[\eta]}$ is equal to a certain eigenmeasure $\rho_{[\eta]}$ with eigenvalue $e^{-\Gamma} = 3^{-\delta}$, conditioned on the rectangles of size $b \times (k-b)$. This measure is of the form*

$$\rho_{[\eta]} = \nu_{\mathrm{Can}}(\mathrm{d}p) \times \nu_{[\eta]}(\mathrm{d}q), \tag{18}$$

where ν_{Can} is the uniform measure (16) on Can*, and $\nu_{[\eta]}$ is a certain probability measure on the interval. $\nu_{[\eta]}$ satisfies the following self-similarity properties:*

(i) for any $0 \leqslant n \leqslant b$ and any sequence $\epsilon_1 \cdots \epsilon_b$ such that $\epsilon_1, \epsilon_2, \ldots, \epsilon_n \in \{0, 2\}$, one has

$$\nu_{[\eta]}([\epsilon_1 \cdots \epsilon_n \cdots \epsilon_b]) = (2 \times 3^\delta)^{-n} \nu_{[\eta]}([\epsilon_{n+1} \cdots \epsilon_b]). \tag{19}$$

(ii) In particular, for any sequence $\epsilon \in \{0, 2\}^n$, the interval $[\epsilon] \subset \mathrm{Can}_n$ has weight $\nu_{[\eta]}([\epsilon]) = (2 \times 3^\delta)^{-n}$. In general, for any b-sequence ϵ containing n symbols $\epsilon_i \neq 1$, we have the upper bound

$$\nu_{[\eta]}([\epsilon]) \leqslant \frac{1}{2^n} \left(\frac{2}{3}\right)^{b-n}. \tag{20}$$

The last bound, together with the definition of ν_{Can}, restricts the concentration of $\rho_{[\eta]}$.

Adapting [31, proposition 8] to the present choice of Walsh quantization, we see that for any fixed primitive sequence η_0 of length k_0, the measure $\rho_{[\eta_0]}$ is the semiclassical limit of the sequence of eigenstates $\left(\Psi^m_{(\eta_0)^n}\right)_{n\to\infty}$, where $m \in \{0, \ldots, k_0 - 1\}$ can vary arbitrarily with n. The above theorem shows that $\rho_{[\eta_0]}$ already coincides, for *finite* k_0, with the averaged Husimi measure (17). In figure 2 we present as an example the spectral average $H^k_{[\eta]}$ for $N = 3^5$ and $\eta = + + + + -$ (equivalently, the measure $\nu_{[\eta]}$ conditioned on the intervals $[\epsilon_1 \cdots \epsilon_5]$).

The next result, which requires much more effort, shows that the measures $\rho_{[\eta]}$ are also relevant to describe the *individual* Husimi measures $H^b_{\Psi^m_\eta}$.

Theorem 3. *Fix a v-square $[\epsilon' \cdot \epsilon]_v$. Take any sequence $\boldsymbol{\eta}$ of length k, any $m \in \{0, \ldots, k-1\}$ and any $b \geqslant v$ such that $k - b \geqslant v$. Then,*

$$H^b_{\Psi^m_\eta}([\epsilon' \cdot \epsilon]_v) = \rho_{[\eta]}([\epsilon' \cdot \epsilon]_v) + \mathcal{O}_v(k^{-1}), \qquad k \to \infty, \tag{21}$$

where $\rho_{[\eta]} = \nu_{\mathrm{Can}} \times \nu_{[\eta]}$ is the eigenmeasure described in theorem 2. The implied constant is independent of $\boldsymbol{\eta}$, m and b.

When considering sequences $\boldsymbol{\eta}$ of lengths $k \to \infty$, any weak-$*$ limit of the measures $(\rho_{[\eta]})$ will be of the form $\nu_{\mathrm{Can}}(\mathrm{d}p) \times \nu(\mathrm{d}q)$ for some probability measure ν on the unit interval. So far all the semiclassical measures we have encountered are of that form. One might wonder whether this is the case for *all* semiclassical measures of the Walsh baker (15). Our last theorem answers this question in the negative.

Theorem 4. *For any $z \in \mathbb{C}$ in the bulk of the nontrivial spectrum (that is, $1/\sqrt{3} < |z| < 1$), there exists an explicit sequence of eigenstates $(\Psi_k)_{k\to\infty}$ with eigenvalues $z_k \to z$, converging to a semiclassical measure ρ which is not of the form $\nu_{\mathrm{Can}}(\mathrm{d}p) \times \nu(\mathrm{d}q)$.*

Remark. In [33] it was noticed that the matrix (15) can also be interpreted as the 'standard' (Weyl-like) quantization of a multivalued symplectic map constructed 'above' the baker's map (7). Within this interpretation, the phase space properties of the eigenstates should be analysed through the *standard* Husimi measures (4) instead of the Walsh–Husimi ones. These two measures generally differ in the vertical (momentum) direction, but their projections $\pi_*\rho$ on the position axis are similar to each other. As a result, for a given sequence of eigenstates (Ψ_k), the semiclassical measures ρ_{stand} obtained as limits of their 'standard' Husimi measures will differ from the Walsh semiclassical measure ρ_{Walsh} described in the theorems above, but their projections on the position axis will be identical. Notice that ρ_{stand} has to be an eigenmeasure of the multivalued baker's map, while ρ_{Walsh} is an eigenmeasure of the (single-valued) open baker's map. For a semiclassical sequence (Ψ_k) with eigenvalues $|z| \to |z_{\max}|$ (respectively $|z| \to |z_{\min}|$), it is not clear whether there is a unique semiclassical measure ρ_{stand}, but in any case the projection $\pi_*\rho_{\mathrm{stand}}$ is unique, equal to ν_{Can} (respectively $\nu_{\min}$).

Theorems 1–4 are our main results. The system we study is the first for which these properties have been proved. It is natural to ask which, if any, of our results extend to quantum chaotic scattering in general. At this stage, the answer to this question is far from being clear, even heuristically, and we consider it to be an interesting avenue for future investigations.

This paper is organized as follows. In the next section we describe the Walsh-baker map in more detail. We prove the exact version of (6), discuss the Walsh-coherent states and the Walsh–Husimi measures. In section 3 we introduce the particular basis of eigenstates $\{\Psi^m_\eta\}$ of the nontrivial spectrum and prove theorems 2 and 3, which involve the study of 'almost periodic' binary sequences (the properties that we need are derived in the appendix). The eigenstates of theorem 4 are exhibited and studied in section 4, while the 'quantum uniqueness' at the edges of the spectrum (theorem 1) is proven in section 5.

2. Walsh quantization of the open baker map

2.1. Walsh kinematics and the open Walsh-baker

In what follows we restrict ourselves to the triadic baker map. A central object in our analysis will be the Cantor set and its generations. Given the interval $\mathrm{Can}_0 = [0, 1)$ the first such generation is $\mathrm{Can}_1 = [0, \frac{1}{3}) \cup [\frac{2}{3}, 1)$, obtained by removing the middle third $[\frac{1}{3}, \frac{2}{3})$, which contains all points of the interval such that their ternary decomposition starts with the digit '1'.

Further generations Can_n are obtained recursively, at each step removing the union of the middle thirds of all the intervals. Therefore Can_n contains all points for which the first n digits in the ternary decomposition take value in $\{0, 2\}$. This process converges to a fractal of Hausdorff dimension $\ln 2/\ln 3$, known as the Cantor set, which we denote by $\mathrm{Can} = \mathrm{Can}_\infty$. This set contains the points in $[0, 1)$, the ternary decomposition of which is made only of the symbols $\{0, 2\}$.

As already mentioned, the allowed position values at the quantum level are of the form $q_j = (j + 1/2)/N$. We only consider the case $N = 3^k$, so that each of the N positions can be labelled by k symbols

$$q_j - \frac{1}{2N} = 0 \cdot \epsilon_1\epsilon_2 \cdots \epsilon_k \quad \text{if } j = \sum_{\ell=1}^{k} \epsilon_\ell\, 3^{k-\ell}, \qquad j \in \{0, \ldots, N-1\}, \quad \epsilon_\ell \in \{0, 1, 2\}. \tag{22}$$

The point q_j belongs to Can_k iff all the $\epsilon_\ell \neq 1$. This ternary decomposition allows position eigenstates $|q_j\rangle$ to be written formally as tensor products,

$$|q_j\rangle = |\epsilon_1\rangle \otimes \cdots \otimes |\epsilon_k\rangle, \qquad \{|\epsilon\rangle,\ \epsilon = 0, 1, 2\} \text{ being the standard basis in } \mathbb{C}^3. \tag{23}$$

This expression takes advantage of the particular structure of the triadic baker map. It is very convenient for addressing the generations of the Cantor set, and constructing the eigenstates of B. The kernel of the Walsh–Fourier transform in the position basis is, for any $j, j' = 0, \ldots, N-1$,

$$(W_N)_{jj'} = 3^{-k/2} \prod_{\ell=1}^{k} \exp\left(-\frac{2\mathrm{i}\pi}{3}(\epsilon_\ell(j) + 1/2)(\epsilon_{k+1-\ell}(j') + 1/2)\right). \tag{24}$$

Equivalently, the action of this transform on tensor product states is given by [32, 33]

$$W_N(v_1 \otimes \cdots \otimes v_k) = F_3 v_k \otimes \cdots \otimes F_3 v_1, \tag{25}$$

where $v_i \in \mathbb{C}^3$ stand for any linear superposition of the basis $\{|\epsilon\rangle,\ \epsilon = 0, 1, 2\}$, and F_3 is the 3×3 matrix defined in (9). Mimicking the 'standard' quantization (8) of the open triadic baker, one gets the matrix (15) as the Walsh quantization of that map. A similar quantization for the closed baker map originally appeared in the context of quantum information [38]. More recently, a wide variety of quantizations of the baker map have been systematically studied [15].

The matrices $B, B^\dagger$ preserve the tensor product decomposition, acting as twisted shifts:

$$B(v_1 \otimes \cdots \otimes v_k) = v_2 \otimes \cdots \otimes v_k \otimes \tilde{F}_3^\dagger v_1, \tag{26}$$

$$B^\dagger(v_1 \otimes \cdots \otimes v_k) = \tilde{F}_3 v_k \otimes v_1 \otimes \cdots \otimes v_{k-1}. \tag{27}$$

Here $\tilde{F}_3$ is the 'open' Fourier transform, obtained by setting to zero the middle row of F_3.

2.2. Spectrum of the open Walsh-baker

The action of the kth iterate B^k is

$$B^k(v_1 \otimes \cdots \otimes v_k) = \tilde{F}_3^\dagger v_1 \otimes \cdots \otimes \tilde{F}_3^\dagger v_k, \tag{28}$$

so we first need to diagonalize the 3×3 matrix $\tilde{F}_3^\dagger$. We call the right eigenvectors of $\tilde{F}_3^\dagger$

$$|f_-\rangle = \frac{1}{\sqrt{2}}(1, 0, -1)^{\mathrm{T}}, \qquad |f_+\rangle = \frac{1}{\sqrt{6}}(1, 2, 1)^{\mathrm{T}}, \qquad |f_0\rangle = (0, 1, 0)^{\mathrm{T}}, \tag{29}$$

the subscripts being inspired by the last entry of the vector. An important property is the *orthogonality* of $|f_-\rangle$ and $|f_+\rangle$, which is specific to the choice of antiperiodic boundary conditions (the choice of periodic boundary conditions yields nonorthogonal vectors [31]). The respective eigenvalues are

$$\lambda_- = 1, \qquad \lambda_+ = \lambda = \frac{i}{\sqrt{3}}, \qquad \lambda_0 = 0. \tag{30}$$

The left eigenvectors of $\tilde{F}_3^\dagger$ are

$$\langle g_-| = \frac{1}{\sqrt{2}}(1, 0, -1), \qquad \langle g_+| = \frac{i}{\sqrt{2}}(1, 0, 1), \qquad \langle g_0| = \frac{i}{\sqrt{3}}(1, -1, 1). \tag{31}$$

Left and right eigenstates are related by

$$F_3|f_0\rangle = |g_0\rangle, \qquad F_3|f_-\rangle = |g_-\rangle, \qquad F_3|f_+\rangle = |g_+\rangle. \tag{32}$$

In particular, we see that the position representation of left eigenstates is equivalent to the momentum representation of right eigenstates. We may thus restrict our attention to right eigenstates only.

The eigenvalues of B^k are obviously given by products of the eigenvalues in (30), and we can make the following sharp distinction between short-lived and long-lived eigenstates:

Convention. *Eigenstates of B corresponding to nonzero eigenvalues are called long-lived, and the remaining ones short-lived.*

The nontrivial spectrum of B^k is spanned by a subspace of dimension 2^k. The $k+1$ eigenvalues $\{\lambda^d : d = 0, \ldots, k\}$ are in general highly degenerate: the multiplicity of λ^d is the binomial coefficient $\binom{k}{d}$. The nonzero eigenvalues of B are then simply of the form $\lambda^{d/k} e^{2\pi i m/k}$ with $0 \leqslant m \leqslant k-1$. The largest one in modulus is $z_{\max} = 1$, while the smallest is $z_{\min} = \lambda = i/\sqrt{3}$. The remaining ones form a lattice inside the annulus $\{|z_{\min}| = 1/\sqrt{3} \leqslant |z| \leqslant z_{\max} = 1\}$, which becomes circular symmetric in the limit $k \to \infty$. No Jordan block appears in the nontrivial spectrum of B.

As noticed in [32, 33], the number of nonzero eigenvalues of B (counted with multiplicities) scales like $N^{\ln 2/\ln 3}$, which corresponds to the fractal Weyl law for this system ($\ln 2/\ln 3$ is half the dimension of the repeller K_0).

2.3. Exact scaling properties of the eigenstates

Let us define the 3×3 'in' and 'out' projectors

$$\pi_I = \begin{pmatrix} 1 & & \\ & 0 & \\ & & 1 \end{pmatrix}, \qquad \pi_O = 1 - \pi_I = \begin{pmatrix} 0 & & \\ & 1 & \\ & & 0 \end{pmatrix}, \tag{33}$$

and the tensor products

$$\Pi_n = \underbrace{\pi_I \otimes \pi_I \otimes \cdots \otimes \pi_I}_{n-1} \otimes \pi_O \otimes \underbrace{1 \otimes \cdots \otimes 1}_{k-n}, \qquad 1 \leqslant n \leqslant k. \tag{34}$$

We see that Π_1 is the projector onto the hole. Let us also define the set of points which fall into the hole after n steps, but not earlier,

$$\mathcal{R}_n = \{x \in O_{-n},\ x \notin O_{-m},\ 0 \leqslant m < n\}, \tag{35}$$

with the convention that $\mathcal{R}_0 = O$. These sets can be written as $\mathcal{R}_n = (\mathrm{Can}_n \setminus \mathrm{Can}_{n+1}) \times [0, 1)$, and are related by

$$\mathcal{U}^{-1}(\mathcal{R}_n) \setminus O = \mathcal{R}_{n+1}. \tag{36}$$

With this definition the projector Π_n corresponds to the region $\mathcal{R}_{n-1}$.

The semiclassical propagation of these projectors is exact up to the Ehrenfest time k, in the sense that $B^\dagger \Pi_n B = \Pi_{n+1}$ for any $n < k$. Indeed, the left-hand side acts as follows on a tensor product state $\boldsymbol{v}$:

$$B^\dagger\, \Pi_n\, B\, \boldsymbol{v} = (\pi_I v_1) \otimes (\pi_I v_2) \cdots (\pi_I v_n) \otimes (\pi_O v_{n+1}) \otimes \cdots \otimes v_k = \Pi_{n+1} \boldsymbol{v}. \tag{37}$$

For any $n \leqslant k$ we thus have $\Pi_n = (B^\dagger)^{n-1} \Pi_1 B^{n-1}$, and the fact that $\Pi_1 = 1 - B^\dagger B$ leads to the relation $\Pi_n = (B^\dagger)^{n-1} B^{n-1} - (B^\dagger)^n B^n$. Let $|\Psi\rangle$ be a normalized right eigenstate of B with eigenvalue z. This state then satisfies

$$\forall n, \quad 0 \leqslant n < k, \qquad \langle \Psi | \Pi_{n+1} | \Psi \rangle = |z|^{2n} (1 - |z|^2), \tag{38}$$

which is the exact version of the general semiclassical property (6).

2.4. Walsh-coherent states

In order to investigate the phase space distribution of the eigenstates of the Walsh quantized open baker map, we use Walsh-coherent states [1, 42] and the associated Walsh–Husimi representations of quantum states. While the usual coherent states are associated with Gaussians in phase space, the 'Walsh' ones are associated with 'quantum rectangles'.

We have been denoting position eigenstates by $|q_j\rangle = |\epsilon_1\rangle \otimes \cdots \otimes |\epsilon_k\rangle$. The action of the Walsh–Fourier transform on these states yields the orthonormal basis of Walsh-momentum eigenstates. Given a certain momentum $p_j = (j + 1/2)/N$, with $j = \epsilon'_1 \epsilon'_2 \cdots \epsilon'_k$ in ternary notation, we associate with p_j the state

$$|p_j\rangle \stackrel{\text{def}}{=} W_N^\dagger |q_j\rangle = F_3^\dagger |\epsilon'_k\rangle \otimes F_3^\dagger |\epsilon'_{k-1}\rangle \otimes \cdots \otimes F_3^\dagger |\epsilon'_1\rangle. \tag{39}$$

As explained in section 1.4, given an integer $0 \leqslant b \leqslant k$, two sequences $\boldsymbol{\epsilon} = \epsilon_1 \cdots \epsilon_b$, $\boldsymbol{\epsilon}' = \epsilon'_1 \cdots \epsilon'_{k-b}$ define a 'quantum rectangle' $[\boldsymbol{\epsilon}' \cdot \boldsymbol{\epsilon}]$ of size $b \times (k - b)$. To this rectangle we associate the Walsh-coherent state $|\boldsymbol{\epsilon}' \cdot \boldsymbol{\epsilon}\rangle_b$:

$$|\boldsymbol{\epsilon}' \cdot \boldsymbol{\epsilon}\rangle_b \stackrel{\text{def}}{=} |\epsilon_1\rangle \otimes \cdots \otimes |\epsilon_b\rangle \otimes F_3^\dagger |\epsilon'_{k-b}\rangle \otimes \cdots \otimes F_3^\dagger |\epsilon'_1\rangle. \tag{40}$$

In particular, for $b = 0$ we recover momentum eigenstates, while $b = k$ corresponds to position eigenstates.

For each choice of $0 \leqslant b \leqslant k$, the family of coherent states $\{|\boldsymbol{\epsilon}' \cdot \boldsymbol{\epsilon}\rangle_b\}$ forms an orthonormal basis of the quantum Hilbert space. Once we select the parameter b, the *Walsh–Husimi measure* associated with a normalized state $|\psi\rangle$ is a probability measure defined through its values on the rectangles of size $b \times (k - b)$:

$$H_\psi^b([\boldsymbol{\epsilon}' \cdot \boldsymbol{\epsilon}]) = |\langle \psi | \boldsymbol{\epsilon}' \cdot \boldsymbol{\epsilon}\rangle_b|^2. \tag{41}$$

In the semiclassical limit a sequence of quantum rectangles can converge to a phase space point only if the parameter b depends on k in such a way that $b(k) \to \infty$ and $k - b(k) \to \infty$. The 'most isotropic' choice consists in taking $b = [k/2]$. Under these conditions, any sequence $(H_{\Psi(k)}^{b(k)})_{k\to\infty}$ admits one or several weak-$*$ limit measures ρ on the torus, and ρ does not depend on the precise choice of b [1].

To study the semiclassical limits, we need to compute the weights of $H_{\Psi(k)}^{b(k)}$ on fixed (that is, k-independent) rectangles, for instance on the family of v-squares $[\boldsymbol{\epsilon}' \cdot \boldsymbol{\epsilon}]_v$ for some fixed

$v \in \mathbb{N}$ (we will sometimes call these squares 'classical' to insist on the independence with respect to k). Let $\Pi_{[\epsilon'\cdot\epsilon]_v}$ denote the projector

$$\Pi_{[\epsilon'\cdot\epsilon]_v} = \pi_{\epsilon_1} \otimes \cdots \pi_{\epsilon_v} \otimes I \cdots I \otimes \tilde{\pi}_{\epsilon'_v} \otimes \cdots \otimes \tilde{\pi}_{\epsilon'_1} \tag{42}$$

(where $\pi_\epsilon = |\epsilon\rangle\langle\epsilon|$, $\tilde{\pi}_\epsilon = F_3^\dagger \pi_\epsilon F_3$) associated with the square $[\epsilon' \cdot \epsilon]_v$. For any parameter $b \geqslant v$ such that $k - b \geqslant v$, the value of the Husimi measure H^b_ψ on $[\epsilon' \cdot \epsilon]_v$ is defined to be

$$H^b_\psi([\epsilon' \cdot \epsilon]_v) = \langle \psi | \Pi_{[\epsilon'\cdot\epsilon]_v} | \psi \rangle. \tag{43}$$

Notice that this is actually independent of b.

Using the fact that $F_3^2 = \begin{pmatrix} & & -1 \\ & -1 & \\ -1 & & \end{pmatrix}$, the Walsh–Fourier transform (24) acts as follows on a coherent state:

$$W_N |\epsilon' \cdot \epsilon\rangle_b = |\epsilon'_1\rangle \otimes \cdots \otimes |\epsilon'_{k-b}\rangle \otimes F_3|\epsilon_b\rangle \otimes \cdots \otimes F_3|\epsilon_1\rangle = (-1)^b \, |\bar{\epsilon} \cdot \epsilon'\rangle_{k-b}, \tag{44}$$

where we defined $\bar{\epsilon}_j = 2 - \epsilon_j$ for all $j = 1, \ldots, b$. The interval indexed by the sequence $\bar{\epsilon}$ is symmetrical (with respect to the origin) to the one indexed by ϵ. Thus, the rectangle $[\bar{\epsilon} \cdot \epsilon']$ is the image of the rectangle $[\epsilon' \cdot \epsilon]$ after a phase space rotation of $\pi/2$ around the origin. We have recovered the Walsh analogue of the action of the Fourier transform F_N on Gaussian coherent states.

The operator B maps b-coherent states into $(b-1)$-coherent states. Indeed, from (26) we have (if $b \geqslant 1$)

$$B|(\epsilon'_{k-b} \cdots \epsilon'_1) \cdot (\epsilon_1 \cdots \epsilon_b)\rangle_b = \delta_{\epsilon_1 \neq 1} |(\epsilon'_{k-b} \cdots \epsilon'_1 \epsilon_1) \cdot (\epsilon_2 \cdots \epsilon_b)\rangle_{b-1}. \tag{45}$$

This action exactly corresponds to the action of the classical open baker map $\tilde{\mathcal{U}}$ on the rectangles $[\epsilon' \cdot \epsilon]$: a rectangle inside the hole ($\epsilon_1 = 1$) is 'killed', while a rectangle outside the hole is transformed classically:

$$B|\epsilon' \cdot \epsilon\rangle_b = \delta_{\epsilon_1 \neq 1} |\mathcal{U}([\epsilon' \cdot \epsilon])\rangle_{b-1}, \qquad \text{and similarly}$$

$$B^\dagger |\epsilon' \cdot \epsilon\rangle_b = \delta_{\epsilon'_1 \neq 1} |\mathcal{U}^{-1}([\epsilon' \cdot \epsilon])\rangle_{b+1}.$$

Let $|\Psi\rangle$ be a long-lived right eigenstate, with $B|\Psi\rangle = z|\Psi\rangle$, $z \neq 0$. Then for any rectangle such that all $\epsilon'_j \neq 1$, we have

$$\forall n \leqslant k - b, \qquad H^b_\Psi([\epsilon' \cdot \epsilon]) = |z|^{-2n} \, H^{b+n}_\Psi(\mathcal{U}^{-n}([\epsilon' \cdot \epsilon])). \tag{46}$$

If on the contrary one of the symbols $\epsilon'_j = 1$, then $H^b_\Psi([\epsilon' \cdot \epsilon]) = 0$. This is the case iff the rectangle $[\epsilon' \cdot \epsilon]$ escapes the system when propagated backwards. The Husimi measure H^b_Ψ is thus supported on $[0, 1) \times \mathrm{Can}_{k-b}$, which can be seen as a coarse-grained version of the backward-trapped set K_+. The concentration of the Husimi function on K_+ was discussed in [8, 23, 31] for the semiclassical limit. The arguments above show that for this system a precise localization already holds for finite k.

The covariance (46) implies the following (Egorov-type) estimate on the weights of v-squares. Assume $k \geqslant 4v$ and take an arbitrary eigenstate Ψ with eigenvalue $z \neq 0$. Its Husimi measure satisfies:

$$H^{[k/2]}_\Psi([\epsilon' \cdot \epsilon]_v) = |z|^{-2v} \left(\prod_{i=1}^{v} \delta_{\epsilon'_i \neq 1} \right) H^{[k/2]}_\Psi([\cdot \epsilon' \epsilon]_{2v}). \tag{47}$$

Hence, to compute the weights of v-squares one only needs to know the weights of 'vertical' rectangles $[\cdot \epsilon' \epsilon]$ of size $2v \times 0$. For actual computations, it will prove convenient to use this property.

3. A particular family of long-lived eigenstates

Let us first describe the short-lived (right) eigenstates of B. From the action of B on tensor products (26), we see that if $\boldsymbol{v} = v_1 \otimes \cdots \otimes v_k$ with $v_1 = |f_0\rangle$ then $B\boldsymbol{v} = 0$. There are $N/3$ such degenerate states, and by taking their overlaps with coherent states we see that they are supported in the hole $\mathcal{R}_0$. If $v_1 \neq |f_0\rangle$ but $v_2 = |f_0\rangle$ then $\boldsymbol{v}$ is not annihilated by the action of B, but we now have $B^2\boldsymbol{v} = 0$, so $\boldsymbol{v}$ is an eigenstate of B in a generalized sense. Since $|f_0\rangle$ appears in the second position, the (Walsh–)Husimi function $H_{\boldsymbol{v}}^b$ of this state is localized in the set $\mathcal{R}_1$. More generally, the Husimi function of a state $\boldsymbol{v}$ such that $B^n\boldsymbol{v} = 0$ and $B^m\boldsymbol{v} \neq 0$ for $0 < m < n$ is supported on the set $\mathcal{R}_{n-1}$ (provided this Husimi function is defined with a parameter $b \geqslant n$).

Hence the short-lived states are supported on classical phase space regions that escape the system before k steps (k corresponds to the Ehrenfest time). In the present system this escape is perfectly deterministic and thus the short-lived states span the generalized kernel of B. For more general systems some unavoidable leakage will lift this degeneracy and lead to small but finite eigenvalues (see [39]).

In the rest of the paper we will focus on the long-lived eigenstates. Since the corresponding eigenspaces are generally quite degenerate, we will choose a particular eigenbasis, which we now describe.

3.1. Construction of the eigenstates $\Psi_{\boldsymbol{\eta}}^m$

As explained in section 1.5, we denote by $\boldsymbol{\eta} = \eta_1\eta_2\cdots\eta_k$, with $\eta_j \in \{+,-\}$, a binary sequence of length k. The number of times the positive sign appears in the sequence $\boldsymbol{\eta}$ is called its *degree* d. The ratio $\delta \stackrel{\text{def}}{=} d/k$ will be called the *relative degree* of $\boldsymbol{\eta}$. With each sequence $\boldsymbol{\eta}$ we associate the state

$$|\boldsymbol{\eta}\rangle = |f_{\eta_1}\rangle \otimes |f_{\eta_2}\rangle \otimes \cdots \otimes |f_{\eta_k}\rangle, \tag{48}$$

where $|f_\pm\rangle$ are the eigenvectors of $\tilde{F}_3^\dagger$ given in (29). The state $|\boldsymbol{\eta}\rangle$ is a right eigenstate of B^k, with the eigenvalue λ^d.

Let τ denote the cyclic shift, such that $\tau\boldsymbol{\eta} = \eta_2\cdots\eta_k\eta_1$. Each sequence has a minimal period $1 \leqslant \ell \leqslant k$ under τ such that $\tau^\ell\boldsymbol{\eta} = \boldsymbol{\eta}$. This period obviously divides k. The orbit of $\boldsymbol{\eta}$ is the set $[\boldsymbol{\eta}] = \{\tau^j\boldsymbol{\eta},\ 0 \leqslant j \leqslant \ell-1\}$ (if $\boldsymbol{\eta}, \boldsymbol{\eta}'$ belong to the same orbit, we will write $\boldsymbol{\eta} \equiv \boldsymbol{\eta}'$). For a given pair ℓ, d there may exist more than one orbit. For example, for $k = 5, d = 2$ the sequences '$++---$' and '$+-+--$' belong to different orbits, both of period $\ell = 5$.

The action of B on $|\boldsymbol{\eta}\rangle$ can be written as $B|\boldsymbol{\eta}\rangle = \lambda_{\eta_1}|\tau\boldsymbol{\eta}\rangle$. Each orbit $[\boldsymbol{\eta}]$ provides us with a family of eigenstates of B. Let us select one representative $\boldsymbol{\eta}$ in this orbit. For any $0 \leqslant m \leqslant \ell-1$ we define $z_{\delta,m/\ell} = \lambda^\delta\,\mathrm{e}^{2\pi\mathrm{i}m/\ell}$ and construct the state

$$|\Psi_{\boldsymbol{\eta}}^m\rangle = \frac{1}{\sqrt{\mathcal{N}}}\sum_{j=0}^{\ell-1}\frac{B^j}{z_{\delta,m/\ell}^j}|\boldsymbol{\eta}\rangle = \frac{1}{\sqrt{\mathcal{N}}}\sum_{j=0}^{\ell-1}c_{jm}|\tau^j\boldsymbol{\eta}\rangle, \tag{49}$$

where

$$c_{jm} = \prod_{s=1}^{j}\frac{\lambda_{\eta_s}}{z_{\delta,m/\ell}}, \qquad c_{0m} = 1 \tag{50}$$

and

$$\mathcal{N} = \sum_{j=0}^{\ell-1}|c_{jm}|^2. \tag{51}$$

This state is a (right) eigenstate of B with eigenvalue $z_{\delta,m/\ell}$. This can be verified by direct inspection. Up to a global phase, it only depends on the orbit $[\boldsymbol{\eta}]$, so with some abuse we may call it $\Psi^m_{[\eta]}$. Notice that $|c_{jm}|$ is independent of m, and so is $\mathcal{N}$. Due to the orthogonality between $|f_-\rangle$ and $|f_+\rangle$, the state $\Psi^m_{[\eta]}$ is normalized, and two states $\Psi^m_{[\eta]}$, $\Psi^{m'}_{[\eta]}$ with $m \neq m'$ are orthogonal to each other. In the same way, eigenstates constructed from different orbits $[\boldsymbol{\eta}] \neq [\boldsymbol{\eta}']$ are also orthogonal to each other. The family

$$\{\Psi^m_{[\eta]}, : [\boldsymbol{\eta}], m = 0, \ldots, \ell(\boldsymbol{\eta}) - 1\}$$

thus forms an orthonormal basis of the nontrivial spectrum of B.

If m, ℓ are coprime, the degeneracy of the eigenvalue $z_{\delta,m/\ell}$ is the number of different orbits with length k, degree d and periods ℓ' such that $\ell|\ell'$ and $\ell'|k$.

3.2. Spectral averages of Husimi measures

In this section we prove theorem 2, which describes spectral averages of Husimi functions of the form (17). Using the eigenfunctions we have constructed, these averages take the form

$$H^b_{[\eta]}([\boldsymbol{\epsilon}' \cdot \boldsymbol{\epsilon}]) = \frac{1}{\mathcal{N}\ell} \sum_{m=0}^{\ell-1} \left| \sum_{j=0}^{\ell-1} \overline{c_{jm}} \langle \tau^j \boldsymbol{\eta} | \boldsymbol{\epsilon}' \cdot \boldsymbol{\epsilon} \rangle_b \right|^2 . \tag{52}$$

For any $0 \leqslant j, j' < \ell$, one has

$$\frac{1}{\ell} \sum_{m=0}^{\ell-1} (z^*_{\delta,m/\ell})^{-j} \, (z_{\delta,m/\ell})^{-j'} = \delta_{j,j'} \, |\lambda|^{-2j\delta}, \tag{53}$$

so that $\sum_{m=0}^{\ell-1} \overline{c_{jm}}\, c_{j'm} = 0$ if $j \neq j'$. Averaging over m thus cancels off-diagonal terms. For any quantum rectangle $[\boldsymbol{\epsilon}' \cdot \boldsymbol{\epsilon}]$ of size $b \times (k - b)$ we find

$$H^b_{[\eta]}([\boldsymbol{\epsilon}' \cdot \boldsymbol{\epsilon}]) = \mathcal{N}^{-1} \sum_{j=0}^{\ell-1} |c_{j0}|^2 \, |\langle \tau^j \boldsymbol{\eta} | \boldsymbol{\epsilon}' \cdot \boldsymbol{\epsilon} \rangle_b|^2. \tag{54}$$

Each overlap on the right-hand side takes the value

$$|\langle \tau^j \boldsymbol{\eta} | \boldsymbol{\epsilon}' \cdot \boldsymbol{\epsilon} \rangle_b|^2 = \prod_{i=1}^{k-b} |\langle \epsilon'_i | g_{\eta_{j-i+1}} \rangle|^2 \prod_{i=1}^{b} |\langle \epsilon_i | f_{\eta_{i+j}} \rangle|^2 \tag{55}$$

(the indices η_{i+j} are extended by periodicity). Let us first study the dependence of $H^b_{[\eta]}([\boldsymbol{\epsilon}' \cdot \boldsymbol{\epsilon}])$ with respect to the momentum coordinate (that is, the symbols ϵ'_i). From expressions (31) for $|g_\pm\rangle$, we immediately see that $|\langle \epsilon'_i | g_{\eta_{j-i+1}} \rangle|^2 = 1/2$ if $\epsilon'_i \neq 1$, and that it vanishes otherwise, independently of $\boldsymbol{\eta}$ or j. The momentum dependence can thus be factorized:

$$H^b_{[\eta]}([\boldsymbol{\epsilon}' \cdot \boldsymbol{\epsilon}]) = \nu_{\mathrm{Can}}([\boldsymbol{\epsilon}']) \, \nu_{[\eta]}([\boldsymbol{\epsilon}]), \tag{56}$$

where

$$\nu_{[\eta]}([\boldsymbol{\epsilon}]) = \mathcal{N}^{-1} \sum_{j=0}^{\ell-1} |c_{j0}|^2 \prod_{i=1}^{b} |\langle \epsilon_i | f_{\eta_{i+j}} \rangle|^2. \tag{57}$$

Here ν_{Can} is the ‘uniform measure’ on Can defined in (16). If we extend formula (57) to sequences $\boldsymbol{\epsilon}$ of arbitrary length, it specifies a probability measure $\nu_{[\eta]}$ on the unit interval, and therefore also a probability measure $\rho_{[\eta]} = \nu_{\mathrm{Can}}(\mathrm{d}p)\, \nu_{[\eta]}(\mathrm{d}q)$ on the torus. The averaged Husimi measure $H^b_{[\eta]}$ is equal to $\rho_{[\eta]}$, conditioned on the rectangles $[\boldsymbol{\epsilon}' \cdot \boldsymbol{\epsilon}]$ of type $b \times (k - b)$. This proves the first statement of theorem 2.

From (54), we see that $\nu_{[\eta]}$ is a convex combination of measures $\nu_{\tau^j\eta}$, where

$$\nu_{\tau^j\eta}([\epsilon_1\cdots\epsilon_b]) = \prod_{i=1}^{b} |\langle\epsilon_i|f_{\eta_{i+j}}\rangle|^2 \tag{58}$$

is a Bernoulli measure associated with the sequence $\tau^j\boldsymbol{\eta}$. $\rho_{[\eta]}$ thus belongs to the class of eigenmeasures studied in [31, proposition 8]; in particular, it is conditionally invariant through the open map $\tilde{\mathcal{U}}$:

$$\tilde{\mathcal{U}}^*\rho_{[\eta]} = |\lambda|^{2\delta}\rho_{[\eta]}. \tag{59}$$

Inserting (59) in the decomposition (56), we obtain the scaling relation (19). Sequences $\boldsymbol{\epsilon} \in \{0,2\}^n$ correspond to intervals of Can_n. The fact that (57) is independent of the choice of the subsequence $\boldsymbol{\epsilon} \in \{0,2\}^n$ shows that the measure $\nu_{[\eta]}$ has the same shape in each connected component of Can_n. From expressions (29) we see that for any b-sequence $\boldsymbol{\epsilon}$ such that exactly n symbols satisfy $\epsilon_i \neq 1$, one has $\nu_{\tau^j\eta}([\boldsymbol{\epsilon}]) \leqslant \frac{1}{2^n}\left(\frac{2}{3}\right)^{b-n}$. The same inequality obviously applies to the convex combination $\nu_{[\eta]}$, which proves (20). This ends the proof of theorem 2.

Through the scaling property (19), we see that the measure $\nu_{[\eta]}$ can be specified by its shape inside the hole (this is a general property of conditionally invariant measures with $\mathrm{e}^{-\Gamma} < 1$ [14]). This shape depends on the specific orbit $[\boldsymbol{\eta}]$. For instance, figure 2 shows the weights $\nu_{[\eta]}([\boldsymbol{\epsilon}])$ for sequences $\boldsymbol{\epsilon}$ of length 5. In that figure, another obvious property of $\nu_{[\eta]}$ is its symmetry with respect to the middle point $q = 1/2$. This property is easy to check in terms of symbolic sequences. For any sequence $\boldsymbol{\epsilon}$, let $\bar{\boldsymbol{\epsilon}}$ be the sequence obtained from $\boldsymbol{\epsilon}$ by replacing everywhere 0 by 2 and vice versa. The interval $[\bar{\boldsymbol{\epsilon}}]$ is exactly the symmetric partner of $[\boldsymbol{\epsilon}]$ with respect to the middle point. Then, one easily checks that for any sequence $\boldsymbol{\epsilon}$, $\nu_{[\eta]}([\bar{\boldsymbol{\epsilon}}]) = \nu_{[\eta]}([\boldsymbol{\epsilon}])$.

3.3. Husimi weights of 'classical rectangles'

In the following sections we will compute Husimi weights of classical rectangles. Keeping $v > 0$ fixed, we select for each $k \geqslant 2v$ an eigenstate Ψ^m_{η} of the form (49). For convenience, we will consider the 'isotropic' Husimi measures $H_\Psi = H_\Psi^{[k/2]}$. As explained before, the sequence $(H_{\Psi^m_\eta})_{k\to\infty}$ has a chance to converge to a semiclassical measure only if the sequences $\boldsymbol{\eta} = \boldsymbol{\eta}(k)$ are chosen such that their relative degrees $\delta(k) \to \delta$.

If the periods $\ell = \ell(k)$ of the sequences $\boldsymbol{\eta}(k)$ are uniformly bounded, we may use the results of [31] to classify the semiclassical measures. Indeed, if $\tilde{\boldsymbol{\eta}}$ is a fixed, primitive sequence, then the Husimi measures associated with the states $\Psi^m_{(\tilde{\eta})^{k'}}$ (with $k' \to \infty$ and $m = m(k')$ arbitrary) converge to the measure $\nu_{\mathrm{Can}}(\mathrm{d}p) \times \nu_{[\tilde{\eta}]}(\mathrm{d}q)$ described in (56) and below. We will thus concentrate here on sequences $\boldsymbol{\eta}(k)$ of periods $\ell(k) \to \infty$.

From the invariance property (47), we may restrict our investigation to the weights of vertical rectangles $[\cdot\boldsymbol{\epsilon}]_v = [\cdot\epsilon_1\cdots\epsilon_v]$. For any primitive k-sequence $\boldsymbol{\eta}$ and any $m \in \{0,\ldots,k-1\}$, the Husimi measure $H_{\Psi^m_\eta}$ of such a vertical rectangle reads

$$H_{\Psi^m_\eta}([\cdot\boldsymbol{\epsilon}]_v) = \mathcal{N}^{-1}\sum_{j,j'=0}^{k-1}\overline{c_{jm}}\,c_{j'm}\langle\tau^j\boldsymbol{\eta}|\Pi_{[\cdot\epsilon]_v}|\tau^{j'}\boldsymbol{\eta}\rangle. \tag{60}$$

Each term (j, j') in the right-hand side of (60) contains the factor

$$\prod_{i=v+1}^{k}\langle f_{\eta_{i+j}}|f_{\eta_{i+j'}}\rangle. \tag{61}$$

From the orthogonality $\langle f_-|f_+\rangle = 0$, this factor vanishes unless the sequences $\tau^j\boldsymbol{\eta}$ and $\tau^{j'}\boldsymbol{\eta}$ coincide along the index set $\{v+1,\ldots,k\}$ (the 'v-bulk'), or equivalently, outside the set $\{1,\ldots,v\}$ (the 'v-box').

If $\boldsymbol{\eta}$ is not primitive, that is if $\boldsymbol{\eta} = \tilde{\boldsymbol{\eta}}^n$ for some primitive $\tilde{\boldsymbol{\eta}}$ and $n > 1$, then as soon as $k \geqslant 2v$ the v-bulk of $\tau^j\boldsymbol{\eta}$ will always contain a *full* sequence $\tau^j\tilde{\boldsymbol{\eta}}$: this implies that the terms $\langle\tau^j\boldsymbol{\eta}|\Pi_{[\cdot\epsilon]_v}|\tau^{j'}\boldsymbol{\eta}\rangle$ vanish if $j \neq j' \bmod \ell$, and one has $H_{\Psi^m_{\eta}}([\cdot\epsilon]_v) = H_{[\eta]}([\cdot\epsilon]_v)$. For this reason we will from now on restrict our attention to eigenstates constructed from long *primitive* sequences $\boldsymbol{\eta}$.

Definition. For $v > 0$ fixed, we take $k \geqslant v$ and consider primitive sequences $\boldsymbol{\eta} = \eta_1\cdots\eta_k$. If there exist two *different* integers $j, j' \in \{0,\ldots,k-1\}$ such that the sequences $\tau^j\boldsymbol{\eta}$ and $\tau^{j'}\boldsymbol{\eta}$ coincide on the v-bulk, then the sequence $\boldsymbol{\eta}$ is said to be (v-)*admissible*. The pair (j, j') is then called an *admissible pair* for $\boldsymbol{\eta}$, and we write $j \overset{v,\eta}{\sim} j'$. Obviously, admissibility is a property of the orbit $[\boldsymbol{\eta}]$.

The Husimi weight (60) can be decomposed into:

$$H_{\Psi^m_{\eta}}([\cdot\epsilon]_v) = \mathcal{N}^{-1}\sum_{j=0}^{k-1}|c_{jm}|^2\langle\tau^j\boldsymbol{\eta}|\Pi_{[\cdot\epsilon]_v}|\tau^j\boldsymbol{\eta}\rangle + \mathcal{N}^{-1}\sum_{j\overset{v,\eta}{\sim}j'}\overline{c_{jm}}\,c_{j'm}\,\langle\tau^j\boldsymbol{\eta}|\Pi_{[\cdot\epsilon]_v}|\tau^{j'}\boldsymbol{\eta}\rangle. \qquad (62)$$

This weight is thus made of 'diagonal' and 'off-diagonal' terms. We have analysed the former in the previous subsection. Our main task will now consist in estimating the contribution of the latter in the cases where it is nontrivial (that is, when $\boldsymbol{\eta}$ is v-admissible).

3.4. *Semiclassical measures of the individual eigenstates* $\Psi^m_{\boldsymbol{\eta}}$

Unlike in the last section, we now fix $v > 0$ and focus on the *individual* Husimi weights $H_{\Psi^m_{\eta}}([\cdot\epsilon]_v)$ given in (62), in the limit $k \to \infty$. The previous section described some properties of the diagonal sum in (62). In this section (which strongly depends on the appendix), we show that the off-diagonal sum in (62) is always negligible in the semiclassical limit, as long as one considers the weights of 'classical' rectangles (that is, take v fixed and $k \to \infty$).

Proposition 1. *Fix $v \geqslant 1$ and take any vertical v-square $[\cdot\epsilon]_v$. Then there exists a constant C_v such that the following holds. For any $k \geqslant 2v$, take a primitive k-sequence $\boldsymbol{\eta}$ and an arbitrary $m \in \{0,\ldots,k-1\}$. One has then:*

$$\left|\mathcal{N}(\boldsymbol{\eta})^{-1}\sum_{j\overset{v,\eta}{\sim}j'}\overline{c_{jm}}\,c_{j'm}\,\langle\tau^j\boldsymbol{\eta}|\Pi_{[\cdot\epsilon]_v}|\tau^{j'}\boldsymbol{\eta}\rangle\right| \leqslant C_v\,k^{-1}. \qquad (63)$$

Before proving this proposition, we briefly explain how it yields theorem 3. If the sequence $\boldsymbol{\eta}$ appearing in theorem 3 is primitive, this is a bound on the off-diagonal sum in (62). As already discussed, if $\boldsymbol{\eta}$ is not primitive and $k \geqslant 2v$ the off-diagonal terms vanish. Besides, the arguments in section 3.2 show that the diagonal terms in (62) yield $\nu_{[\eta]}([\cdot\epsilon]_v)$, so we get (21) in the case of vertical v-rectangles. Finally, from the Egorov property (47) the same equation holds if we replace a vertical $2v$-rectangle by a v-square $[\epsilon'\cdot\epsilon]_v$.

Proof of the proposition. The results of section 3.3 show that the right-hand side in (63) can be nonvanishing only if the k-sequence $\boldsymbol{\eta}$ is v-admissible. Among the full set of primitive sequences of length k, admissible sequences constitute a very restricted set: even though they are primitive, these sequences are *almost periodic*, and have a rich hierarchical structure, described in the appendix. We now describe some features of this almost-periodic structure, relevant for our aims.

3.4.1. Hierarchical structure of admissible sequences. Fix $v > 0$ and $k \gg v$. The analysis of the appendix classifies the family of v-admissible binary sequences (which are primitive of length k) according to their *rank*, which is a positive integer $n \leqslant \log_2 k$. The rank describes the number of *levels* used to encode the hierarchical structure of the sequence.

A v-admissible sequence of rank n will be a repetition of two 'elementary strings', which we will denote by R_n and D_n. The letters R, D are for 'Repeated' versus 'Defect', while the subscript n means that these strings correspond to the 'nth level' of $\boldsymbol{\eta}$. The strings D_n, R_n have lengths $\leqslant v$, and they cannot be of the form $R_n = (\tilde{\boldsymbol{\eta}})^m$, $D_n = (\tilde{\boldsymbol{\eta}})^{m'}$, that is repetitions of a common string $\tilde{\boldsymbol{\eta}}$. We believe that the strings D_n, R_n satisfy further constraints, but we do not need to know these explicitly for our purposes.

To construct the full sequence $\boldsymbol{\eta}$ starting from the two strings R_n, D_n, one proceeds iteratively from level n down to level 1. The construction is encoded by a sequence of n signed integers

$$(\sigma_1 r_1, \sigma_2 r_2, \ldots, r_n), \qquad \text{with } r_i \geqslant 2,\ \sigma_i \in \{\pm\}. \tag{64}$$

Starting from $j = n$ down to $j = 1$, we use the two level-j strings D_j, R_j to construct the 'long' and 'short' strings at level $j-1$ by the following concatenations:

$$\begin{pmatrix} L_{j-1} \\ S_{j-1} \end{pmatrix} \stackrel{\text{def}}{=} \begin{pmatrix} D_j\, R_j^{r_j} \\ D_j\, R_j^{r_j-1} \end{pmatrix}. \tag{65}$$

One of these two level-$(j-1)$ strings will be the 'defect', the other one being the 'repeated string'; the choice depends on the sign σ_j:

$$\forall j = 2, \ldots, n, \qquad \begin{cases} D_{j-1} = L_{j-1},\ R_{j-1} = S_{j-1} & \text{if } \sigma_{j-1} = +, \\ D_{j-1} = S_{j-1},\ R_{j-1} = L_{j-1} & \text{if } \sigma_{j-1} = -. \end{cases} \tag{66}$$

Finally, the k-sequence $\boldsymbol{\eta}$ is given (up to a global shift) by

$$\boldsymbol{\eta} \equiv D_1\, R_1^{r_1-1}.$$

The analysis of the appendix shows that, for each $j \leqslant n-1$, the level-j strings R_j, D_j are necessarily primitive.

3.4.2. Two properties of admissible sequences. To estimate the left-hand side of (63), our first objective is to count the number of admissible pairs $j \stackrel{v,\eta}{\sim} j'$ (we recall that $j \sim j'$ implies that $j \neq j'$). This counting is done in appendix A.3.1 of the appendix, and leads to the following

Proposition 2. *There exists $C > 0$ such that the following estimate holds. Fix $v > 0$. For any length $k > v$ and any primitive sequence $\boldsymbol{\eta}$ of length k, the number of admissible pairs $j \stackrel{v,\eta}{\sim} j'$ is bounded from above by $C\,v^2$.*

The number of terms in (63) is thus uniformly bounded when $k \to \infty$. It remains to control the variations of the coefficients $c_{jm}(\boldsymbol{\eta})$ (defined in (51)), and the size of $\mathcal{N}(\boldsymbol{\eta})$. This is done in appendix A.4 of the appendix, and leads to

Proposition 3. *Call $\Lambda = -\log|\lambda| = \frac{1}{2}\log 3$. For any v-admissible sequence $\boldsymbol{\eta}$ of length $k > v$, any $m \in \{0, \ldots, k-1\}$ and any ℓ, the coefficients $c_{jm}(\tau^\ell \boldsymbol{\eta})$ satisfy*

$$-3v\Lambda \leqslant \log|c_{jm}(\tau^\ell \boldsymbol{\eta})| \leqslant 3v\Lambda, \qquad j = 1, \ldots, k. \tag{67}$$

Notice that these bounds are not satisfied by all k-sequences (see for instance the sequences used in section 4). They are a consequence of the almost-periodicity of $\boldsymbol{\eta}$. These bounds straightforwardly imply the following estimates for the normalization factor $\mathcal{N}(\boldsymbol{\eta})$:

$$|\lambda|^{6v}\, k \leqslant \mathcal{N}(\boldsymbol{\eta}) \leqslant |\lambda|^{-6v}\, k.$$

Using proposition 2 we get, for any v-admissible k-sequence (and thus, trivially, for any primitive k-sequence):

$$\mathcal{N}^{-1} \sum_{j \overset{v,\eta}{\sim} j'} |\overline{c_{jm}}\, c_{j'm}\, \langle \tau^j \boldsymbol{\eta} | \Pi_{[\cdot\epsilon]_v} | \tau^{j'} \boldsymbol{\eta} \rangle| \leqslant \mathcal{N}^{-1} \sum_{j \overset{v,\eta}{\sim} j'} |c_{jm}\, c_{j'm}| \leqslant C\, v^2\, |\lambda|^{-12v}\, k^{-1}.$$

This ends the proof of proposition 1, and thus of theorem 3. □

This theorem strongly constrains the semiclassical measures one can obtain from a family $(\Psi_{\eta}^m)_{k\to\infty}$, where $\boldsymbol{\eta} = \boldsymbol{\eta}(k)$ and $m = m(k)$ are chosen arbitrarily. From [31] we know that, if such a family converges to a semiclassical measure ρ with decay rate $\mathrm{e}^{-\Gamma}$, then the corresponding eigenvalues $|z_{\delta(k),m/k}| \to \mathrm{e}^{-\Gamma/2}$, which means that the relative degrees of the sequences $\boldsymbol{\eta}(k)$ converge towards $\frac{\Gamma}{\log 3}$. The limit measure is then of the form $\rho = \nu_{\mathrm{Can}}(\mathrm{d}p) \times \nu(\mathrm{d}q)$, with ν being the limit of the measures $\nu_{[\eta(k)]}$. Although such limits ν can be quite diverse, they will necessarily satisfy the properties of $\nu_{[\eta(k)]}$ described in theorem 2.

In the following section we exhibit semiclassical measures which are *not* of the above type.

4. Combination of two eigenstates Ψ_{η}^m

In this section we prove theorem 4, that is we provide examples of semiclassical measures which are not of the form $\nu_{\mathrm{Can}}(\mathrm{d}p) \times \nu(\mathrm{d}q)$. These measures will be associated with linear combinations of two particular degenerate eigenstates $\Psi_{\eta}^m, \Psi_{\eta'}^m$.

Fix some complex number z with $|\lambda| < |z| < 1$. For any integer $k > 1$, we can choose a degree $d = d(k) \in \{1, \ldots, k-1\}$ and $m = m(k) \in \{0, \ldots, k-1\}$, such that the eigenvalues

$$z_{\delta(k),m/k} \overset{k\to\infty}{\longrightarrow} z, \qquad \text{that is,} \quad \frac{d(k)}{k} \to \delta(\infty) = \frac{\log|z|}{\log|\lambda|}, \quad \frac{m(k)}{k} \to \frac{\arg(z/\lambda^{\delta(\infty)})}{2\pi}. \tag{68}$$

For each $k > 4$, we then consider the two following k-sequences, which we choose to label by indices $-k+d+1, \ldots, d$:

$$\boldsymbol{\eta} = \eta_{-k+d+1} \cdots \eta_d = (-)^{k-d}(+)^d, \qquad \boldsymbol{\eta}' = \eta'_{-k+d+1} \cdots \eta'_d = (-)^{k-d-1} + - (+)^{d-1}. \tag{69}$$

These sequences have the same relative degree, and are primitive.

Proposition 4. *Consider the two eigenstates Ψ_{η}^m, $\Psi_{\eta'}^m$ constructed from the sequences (69), satisfying the condition (68). Fix $\alpha, \alpha' \in \mathbb{C}$ such that $|\alpha|^2 + |\alpha'|^2 = 1$.*

Then, the sequence of eigenstates $(\alpha\Psi_{\eta}^m + \alpha'\Psi_{\eta'}^m)_{k\geqslant 1}$ converges to a semiclassical measure $\mu_{\alpha,\alpha'}$. If $\Im(\bar{\alpha}\alpha') \neq 0$, this measure is not of the type $\nu_{\mathrm{Can}}(\mathrm{d}p) \times \nu(\mathrm{d}q)$.

proof. Let us first study the limit measure of the sequence (Ψ_{η}^m). One can easily check that for $d \geqslant 2v$ and $k - d \geqslant 2v$ the sequence $\boldsymbol{\eta}$ is not v-admissible. Thus, from the results of the previous sections, the Husimi weight of any v-square is given by

$$H_{\Psi_{\eta}^m}([\epsilon' \cdot \epsilon]_v) = \frac{1}{\mathcal{N}} \sum_{j=-k+d+1}^{d} |c_{j0}|^2\, \langle \tau^j \boldsymbol{\eta} | \Pi_{[\epsilon'\cdot\epsilon]_v} | \tau^j \boldsymbol{\eta} \rangle = \nu_{\mathrm{Can}}([\epsilon']_v) \times \nu_{[\eta]}([\epsilon]_v). \tag{70}$$

An explicit computation of the coefficients $c_{j0}(\boldsymbol{\eta})$ gives

$$(c_{j0}(\boldsymbol{\eta}))_{j=-k+d+1,\ldots,d} = (\lambda^{(k-d-1)\delta}, \ldots, \lambda^{2\delta}, \lambda^{\delta}, 1, \lambda^{(1-\delta)}, \lambda^{2(1-\delta)}, \ldots, \lambda^{d(1-\delta)}). \tag{71}$$

If we extend the sequence $\boldsymbol{\eta}$ in (69) to a bi-infinite sequence in 'the obvious way' (that is, taking $\eta_j = +$ for $j > d$ and $\eta_j = -$ for $j < -k+d+1$), and similarly extend the coefficients $|c_{j0}|^2$ using the two geometric progressions, then the extension of the sum in (70) to $j \in \mathbb{Z}$ yields the weight of a certain measure $\rho_{\delta(k)} = \nu_{\text{Can}} \times \nu_{\delta(k)}$, which is an exact eigenmeasure of $\mathcal{U}$ of eigenvalue $|\lambda|^{2\delta(k)}$. Due to the geometric decrease, the difference between the two measures is small:

$$\nu_{\delta(k)}([\boldsymbol{\epsilon}]_v) = \nu_{[\eta]}([\boldsymbol{\epsilon}]_v) + \mathcal{O}_v(|\lambda|^{\delta(1-\delta)k}), \qquad k \to \infty.$$

In the limit $\delta(k) \to \delta(\infty)$, the measure $\nu_{\delta(k)}$ converges to the eigenmeasure $\nu_{\delta(\infty)}$.

A similar computation shows that the Husimi measure $H_{\Psi^m_{\eta'}}$ is close to an eigenmeasure $\rho'_{\delta(k)} = \nu_{\text{Can}}(\text{d}p) \times \nu'_{\delta(k)}(\text{d}q)$, which converges to $\rho'_{\delta(\infty)}$ when $\delta(k) \to \delta(\infty)$.

Now, let us consider $\Psi_k \stackrel{\text{def}}{=} \alpha\Psi^m_{\boldsymbol{\eta}} + \alpha'\Psi^m_{\boldsymbol{\eta}}$, with $|\alpha|^2 + |\alpha'|^2 = 1$. In the equation

$$H_{\Psi_k}([\boldsymbol{\epsilon}'\cdot\boldsymbol{\epsilon}]_v) = |\alpha|^2\, H_{\Psi^m_{\eta}}([\boldsymbol{\epsilon}'\cdot\boldsymbol{\epsilon}]_v) + |\alpha'|^2\, H_{\Psi^m_{\eta'}}([\boldsymbol{\epsilon}'\cdot\boldsymbol{\epsilon}]_v) + 2\Re(\bar{\alpha}\alpha'\langle\Psi^m_{\boldsymbol{\eta}}|\Pi_{[\epsilon'\cdot\epsilon]_v}|\Psi^m_{\boldsymbol{\eta}'}\rangle),$$

we need to control the cross-term, which is a linear combination of overlaps $\langle\tau^j\boldsymbol{\eta}|\Pi_{[\epsilon'\cdot\epsilon]_v}|\tau^{j'}\boldsymbol{\eta}'\rangle$. From the structures of $\boldsymbol{\eta}$ and $\boldsymbol{\eta}'$ this overlap is nonvanishing only if $j = j' \in \{-v+1, \ldots, v-1\}$. Thus, the cross-term amounts to the finite sum

$$\frac{2}{\sqrt{\mathcal{N}(\boldsymbol{\eta})\,\mathcal{N}(\boldsymbol{\eta}')}}\,\Re\left(\bar{\alpha}\alpha' \sum_{j=-v+1}^{v-1} \overline{c_{j0}(\boldsymbol{\eta})}\, c_{j0}(\boldsymbol{\eta}')\langle\tau^j\boldsymbol{\eta}|\Pi_{[\epsilon'\cdot\epsilon]_v}|\tau^j\boldsymbol{\eta}'\rangle\right).$$

From the geometric decay of the coefficients c_{j0}, this sum takes the form $\mu_{\text{off},\delta(\text{k})}([\boldsymbol{\epsilon}'\cdot\boldsymbol{\epsilon}]_v) + \mathcal{O}(|\lambda|^{\delta(1-\delta)k})$, where $\mu_{\text{off},\delta}$ is a signed measure (that is, the difference between two positive measures) which is conditionally invariant under $\tilde{\mathcal{U}}$. In the case of a square $[\epsilon'_1\cdot\epsilon_1]_1$, the above sum reduces to a single term $j = 0$:

$$\overline{c_{00}(\boldsymbol{\eta})}\, c_{00}(\boldsymbol{\eta}')\langle f_+|\epsilon_1\rangle\langle\epsilon_1|f_-\rangle\langle g_-|\epsilon'_1\rangle\langle\epsilon'_1|g_+\rangle = \begin{cases} -i/4\sqrt{3}, & \epsilon_1 = \epsilon'_1 \in \{0,2\},\\ i/4\sqrt{3}, & \epsilon_1 \neq \epsilon'_1 \in \{0,2\},\\ 0 & \text{otherwise.}\end{cases}$$

Thus, if $\Im(\bar{\alpha}\alpha') \neq 0$, we see that the signed measure $\mu_{\text{off},\delta}$ cannot be factorized into the form $\nu_{\text{Can}}(\text{d}p) \times \nu_{\text{off},\delta}(\text{d}q)$. Hence, the semiclassical measure $\mu_{\alpha,\alpha'} = |\alpha|^2\rho_{\delta(\infty)} + |\alpha'|^2\rho'_{\delta(\infty)} + \mu_{\text{off},\delta(\infty)}$ is not of that form either. □

5. QUE at the edges of the spectrum

In the preceding sections we considered semiclassical measures with eigenvalues in the 'bulk' of the nontrivial spectrum, $|z|^2 \in (1/3, 1)$. In this section, we restrict ourselves to eigenstates of eigenvalues $z_{\delta,m}$ situated close to the *edges* of the nontrivial spectrum, that is the circles $\{|z| = 1\}$ and $\{|z| = 1/\sqrt{3}\}$. Since the analysis of the two cases is very similar, we will mostly focus on the outer edge, that is the vicinity of the unit circle. The eigenvalues $z_{\delta,m/\ell}$ satisfy $|z_{\delta,m/\ell}| = |\lambda|^\delta = 1 + \mathcal{O}(\delta)$, so they will approach the unit circle iff the relative degrees

$$\delta(k) \to 0 \qquad \text{as } k \to \infty. \tag{72}$$

The general eigenstate of $z_{\delta,m/\ell}$ is a linear combination of eigenstates $\Psi^m_{\boldsymbol{\eta}}$ constructed from sequences $\boldsymbol{\eta} = \boldsymbol{\eta}(k)$ of the same relative degree $\delta(k)$. Notice that the periods $\ell(k)$ of $\boldsymbol{\eta}(k)$ satisfy $\ell \geqslant \delta^{-1}$, so they necessarily diverge when $k \to \infty$.

5.1. *Individual states Ψ_{η}^{m} at the outer edge of the spectrum*

As a first step towards the proof of theorem 1, we consider the semiclassical measures associated with a family $(\Psi_{\eta}^{m})_{k\to\infty}$ satisfying (72). From proposition 1, we are reduced to studying the limits of the associated measures $\nu_{[\eta]}$.

Proposition 5. *Consider sequences $(\boldsymbol{\eta} = \boldsymbol{\eta}(k))_{k\to\infty}$ such that the relative degrees $\delta(k) \to 0$ and their associated measures $\nu_{[\eta(k)]}$ (see (57)). Then, for any fixed subinterval $[\epsilon_1 \cdots \epsilon_v]$, we have*

$$\nu_{[\eta(k)]}([\boldsymbol{\epsilon}]) = \nu_{\mathrm{Can}}([\boldsymbol{\epsilon}]) + \mathcal{O}_v(\delta(k)),$$

where ν_{Can} is the uniform measure on the Cantor set (see (16)).

As a consequence, the semiclassical measure associated with a family $(\Psi_{\eta(k)}^{m(k)})_{k\to\infty}$ is $\rho_{\max} = \nu_{\mathrm{Can}}(\mathrm{d}p) \times \nu_{\mathrm{Can}}(\mathrm{d}q)$.

Proof. From the discussion in section 3.3, it is sufficient to prove the proposition for primitive k-sequences $\boldsymbol{\eta}$. A sequence $\boldsymbol{\eta}$ of relative degree $\delta(k) \ll 1$ will contain many more minuses than pluses. It thus makes sense to split the sum in (57) between the indices j such that the v-box of $\tau^j\boldsymbol{\eta}$ contains *only minuses*, and the indices j for which the v-box contains at least one plus. We write this decomposition as

$$\nu_{[\eta]}([\boldsymbol{\epsilon}]) = \mathcal{N}^{-1}\sum_{j}^{(-)} |c_{j0}|^2 \prod_{i=1}^{v} |\langle \epsilon_i | f_- \rangle|^2 + \mathcal{N}^{-1}\sum_{j}^{(+)} |c_{j0}|^2 \prod_{i=1}^{v} |\langle \epsilon_i | f_{\eta_{i+j}} \rangle|^2. \tag{73}$$

Our aim is to show that the second term on the right hand side becomes small when $k \to \infty$ and $\delta(k) \to 0$. This will result from two facts. Firstly, since there are $\delta(k)k$ pluses in $\boldsymbol{\eta}$, the number of terms in $\sum^{(+)}$ is bounded from above by $v\,\delta(k)\,k$, which is much smaller than the number of terms in $\sum^{(-)}$ (larger than $k(1 - v\,\delta(k))$).

Then, we also need to control precisely the variations of the coefficients $|c_{j0}(\boldsymbol{\eta})|$ (which we will denote by $|c_j|$ for short). These variations can be more easily visualized by considering the logarithms

$$B_j(\boldsymbol{\eta}) \stackrel{\text{def}}{=} \log|c_j(\boldsymbol{\eta})| = \sum_{s=1}^{j} \log\left|\frac{\lambda_{\eta_s}}{\lambda^{\delta}}\right|. \tag{74}$$

The sequence $(B_j)_{j=0,\dots,k}$ accomplishes a discrete path with endpoints at the origin and two kinds of steps:

$$B_{j+1}(\boldsymbol{\eta}) - B_j(\boldsymbol{\eta}) = \begin{cases} \delta\Lambda > 0 & \text{if } \eta_{j+1} = (-) \\ (\delta - 1)\Lambda < 0 & \text{if } \eta_{j+1} = (+), \end{cases} \qquad \Lambda = \log|1/\lambda|. \tag{75}$$

For $\delta \ll 1$, the path will be made of many small ups and few steep downs. Let us call $\{j_1 < j_2 < \cdots < j_d\}$ the indices such that $\eta_{j_r+1} = (+)$, and take $\ell_r = j_r - j_{r-1}$, so that η_{j_r+1} is preceded by a substring $(-)^{\ell_r-1}$. Grouping together $|c_{j_r}|^2$ with the coefficients along the preceding substring, the normalization factor can be written as

$$\mathcal{N}(\boldsymbol{\eta}) = \sum_{r=1}^{d} C_r, \qquad C_r \stackrel{\text{def}}{=} |c_{j_r}|^2 \sum_{m=0}^{\ell_r-1} |\lambda|^{2m\delta} = |c_{j_r}|^2 \frac{1 - |\lambda|^{2\delta\ell_r}}{1 - |\lambda|^{2\delta}}. \tag{76}$$

We now split the above sum between the 'long' and 'short' ℓ_r. We fix some $\varepsilon \in (0, 1/4)$ (independent of δ), and consider the subsets of indices

$$\mathcal{L} \stackrel{\text{def}}{=} \{r \in [1, d] \; : \; \ell_r > \varepsilon/\delta\}, \qquad \mathcal{S} \stackrel{\text{def}}{=} [1, d] \setminus \mathcal{L}.$$

One sees from (75) that any index $j_{\max}$ at which B_j reaches its maximum is necessarily of the form $j_{\max} = j_r$ for some $r \in \mathcal{L}$. Conversely, for any $r \in \mathcal{L}$, the coefficient B_{j_r} is a 'local maximum', in the sense that $B_{j_r} > B_{j_r-1}$ and $B_{j_r} > B_{j_r+1}$. We will show that the sum (76) is controlled by the 'long' coefficients j_r:

Lemma 1. *Consider the same assumptions as in proposition 5, and fix some $\varepsilon > 0$. Then there is a constant $C_\varepsilon > 0$ such that, for δ small enough,*

$$C_\varepsilon^{-1}\,\delta^{-1}\sum_{r\in\mathcal{L}}|c_{j_r}|^2 \leqslant \mathcal{N}(\boldsymbol{\eta}) \leqslant C_\varepsilon\,\delta^{-1}\sum_{r\in\mathcal{L}}|c_{j_r}|^2.$$

Proof. We first estimate the contribution of 'long' substrings to the sum (76):

$$\forall r\in\mathcal{L},\qquad c'_\varepsilon\,\delta^{-1}\,|c_{j_r}|^2 \geqslant |c_{j_r}|^2\,\frac{1}{1-|\lambda|^{2\delta}} \geqslant C_r \geqslant |c_{j_r}|^2\,\frac{1-|\lambda|^{2\varepsilon}}{1-|\lambda|^{2\delta}} \geqslant c_\varepsilon\,\delta^{-1}\,|c_{j_r}|^2. \tag{77}$$

From (50) we have that $|c_{j_r}| = |c_{j_{r-1}}||\lambda|^{1-\delta\ell_r}$. We then check that

$$\forall r\in\mathcal{S},\qquad C_r \leqslant |c_{j_r}|^2\,\frac{1-|\lambda|^{2\varepsilon}}{1-|\lambda|^{2\delta}}\quad\text{and}\quad |\lambda|^{1-\delta}\leqslant\frac{|c_{j_r}|}{|c_{j_{r-1}}|}\leqslant|\lambda|^{1-\varepsilon}. \tag{78}$$

The set of indices $\mathcal{S}$ can be represented as a disjoint union of 'discrete intervals':

$$\mathcal{S} = \bigsqcup_s I_s,\quad\text{where } I_s = \{j \mid r_s \leqslant j \leqslant r_s + l_s - 1\}\qquad\text{and}\qquad r_s + l_s < r_{s+1}.$$

We are denoting by l_s the length of the discrete interval I_s and by r_s its starting point. Using the inequalities (78), we see that the contribution of each interval I_s to $\sum_r C_r$ is controlled by j_{r_s-1}, which is the first 'long' index at the left of I_s:

$$\sum_{r\in I_s}|c_{j_r}|^2 \leqslant |c_{j_{r_s-1}}|^2\,|\lambda|^{2(1-\varepsilon)}\,\frac{1-|\lambda|^{2(1-\varepsilon)l_s}}{1-|\lambda|^{2(1-\varepsilon)}} \leqslant C\,|c_{j_{r_s-1}}|^2. \tag{79}$$

Taking (77) into account, we see that the sum (76) is of the order of $\delta^{-1}\sum_{r\in\mathcal{L}}|c_{j_r}|^2$. □

Any index j in the sum $\Sigma^{(+)}$ is necessarily at distance $\leqslant v$ from some index j_r (because the interval $[j-v, j+v]$ necessarily contains a (+)), which implies $|c_j| \leqslant |\lambda|^{-v}|c_{j_r}|$. We thus get

$$\sum_j^{(+)}|c_j|^2 \leqslant C\sum_{r=1}^{d}|c_{j_r}|^2 \leqslant C'\sum_{r\in\mathcal{L}}|c_{j_r}|^2.$$

We used equation (79) in the last inequality. Applying lemma 1, we obtain the following upper bound for the second sum in (73):

$$\mathcal{N}^{-1}\sum_j^{(+)}|c_j|^2 = \mathcal{O}(\delta),\qquad \delta\to 0. \tag{80}$$

This implies the following estimate for the complementary sum:

$$\mathcal{N}^{-1}\sum_j^{(-)}|c_j|^2 = 1 - \mathcal{N}^{-1}\sum_j^{(+)}|c_j|^2 = 1 + \mathcal{O}(\delta).$$

The proof of the proposition is achieved by noticing that $\prod_{i=1}^{v}|\langle\epsilon_i|f_-\rangle|^2 = \nu_{\mathrm{Can}}([\boldsymbol{\epsilon}])$. □

5.2. General eigenstates at the outer edge of the spectrum

To prove the first part of theorem 1, we need to consider arbitrary eigenstates, which are linear combinations of the states Ψ_η^m.

For z inside the unit disc, we call $\mathcal{C}_k(z)$ the set of orbits $[\boldsymbol{\eta}]$, such that $\boldsymbol{\eta}$ is a k-sequence of relative degree δ, and there exists $m \in \{0, \ldots, \ell(\boldsymbol{\eta}) - 1\}$ such that $z_{\delta,m/\ell} = z$ (we will only consider the case where $\mathcal{C}_k(z)$ is nonempty). We notice that the periods of two orbits $[\boldsymbol{\eta}],\ [\boldsymbol{\eta}'] \in \mathcal{C}_k(z)$ may differ. On the other hand, with a given orbit $[\boldsymbol{\eta}] \in \mathcal{C}_k(z)$ is associated a single integer $m \in \{0, 1, \ldots, \ell - 1\}$ such that $z_{\delta,m/\ell} = z$. The states $\{\Psi_{\boldsymbol{\eta}}^m,\ [\boldsymbol{\eta}] \in \mathcal{C}_k(z)\}$ form an orthonormal basis of the z-eigenspace, so a general z-eigenstate will be written

$$|\Psi\rangle = \sum_{[\eta]\in\mathcal{C}_k(z)} d_\eta |\Psi_\eta^m\rangle, \quad d_\eta \in \mathbb{C}, \qquad \sum_{[\eta]\in\mathcal{C}_k(z)} |d_\eta|^2 = 1.$$

For $k \gg v$, the Husimi measure of a vertical rectangle $[\cdot\boldsymbol{\epsilon}]_v$ reads:

$$H_\Psi([\cdot\boldsymbol{\epsilon}]_v) = \sum_{[\eta],[\eta']\in\mathcal{C}_k(z)} \overline{d_{\eta'}}\, d_\eta\, \langle \Psi_{\eta'}^{m'} | \Pi_{[\cdot\epsilon]_v} | \Psi_\eta^m \rangle. \tag{81}$$

The diagonal matrix elements can be estimated using proposition 5:

$$\sum_{[\eta]\in\mathcal{C}_k(z)} |d_\eta|^2 H_{\Psi_\eta^m}([\cdot\boldsymbol{\epsilon}]_v) = \rho_{\max}([\cdot\boldsymbol{\epsilon}]_v) + \mathcal{O}_v(\delta), \tag{82}$$

uniformly with respect to the normalized vector (d_η).

We now want to estimate the off-diagonal terms in (81). For two orbits $[\boldsymbol{\eta}] \neq [\boldsymbol{\eta}']$ in $\mathcal{C}_k(z)$, we will write $[\boldsymbol{\eta}] \overset{v}{\sim} [\boldsymbol{\eta}']$ if there exists $(j, j') \in \mathbb{Z}/\ell\mathbb{Z} \times \mathbb{Z}/\ell'\mathbb{Z}$ such that $\tau^j\boldsymbol{\eta}$ and $\tau^{j'}\boldsymbol{\eta}'$ coincide in the v-bulk. This is possible only if the v-box of $\tau^j\boldsymbol{\eta}$ contains some pluses, and $\tau^{j'}\boldsymbol{\eta}'$ consists in a reshuffling of these pluses inside the box. For any k-orbit $\boldsymbol{\eta}$, we call $\mathrm{resh}(\boldsymbol{\eta})$ the set of k-sequences which coincide with $\boldsymbol{\eta}$ in the v-bulk and have the same degree as $\boldsymbol{\eta}$. Obviously, $\#\mathrm{resh}(\boldsymbol{\eta}) \leqslant v!$.

We define the following Hermitian matrix, indexed by the orbits $[\boldsymbol{\eta}] \in \mathcal{C}_k(z)$:

$$M_{[\eta'],[\eta]} \overset{\text{def}}{=} \begin{cases} \langle \Psi_{\eta'}^{m'} | \Pi_{[\cdot\epsilon]_v} | \Psi_\eta^m \rangle, & [\boldsymbol{\eta}'] \neq [\boldsymbol{\eta}], \\ 0, & [\boldsymbol{\eta}'] = [\boldsymbol{\eta}]. \end{cases} \tag{83}$$

Observe that off-diagonal elements vanish unless $[\boldsymbol{\eta}] \overset{v}{\sim} [\boldsymbol{\eta}']$. Our aim is to estimate the *spectral radius* of this matrix, $r_{\mathrm{sp}}(M)$. If $\|v\|_\infty = \max_{[\eta]} |v_{[\eta]}|$ is the sup-norm in the vector space of dimension $\#\mathcal{C}_k(z)$, then the corresponding norm of the matrix M is given by

$$\|M\|_\infty = \max_{[\eta]} M_{[\eta]}, \qquad \text{where } M_{[\eta]} = \sum_{[\eta']\in\mathcal{C}_k(z)} |M_{[\eta],[\eta']}|.$$

This norm $\|M\|_\infty$ is necessarily greater than or equal to the spectral radius $r_{\mathrm{sp}}(M)$. For each $[\boldsymbol{\eta}]$, the sum $M_{[\eta]}$ takes the form

$$M_{[\eta]} = \sum_{[\eta']\overset{v}{\sim}[\eta]} |\langle \Psi_{\eta'}^{m'} | \Pi_{[\cdot\epsilon]_v} | \Psi_\eta^m \rangle| \,. \tag{84}$$

Using the above remarks on the sequences $[\boldsymbol{\eta}'] \overset{v}{\sim} [\boldsymbol{\eta}]$, and calling $\{j_r\}$ the indices such that $\eta_{j_r+1} = (+)$, we find

$$M_{[\eta]} \leqslant \mathcal{N}(\boldsymbol{\eta})^{-1/2} \sum_{r=1}^{d} \sum_{j:|j-j_r|\leqslant v} |c_j(\boldsymbol{\eta})| \sum_{\tilde{\eta}\in\mathrm{resh}(\tau^j\eta)} \mathcal{N}(\tilde{\boldsymbol{\eta}})^{-1/2}\, |c_0(\tilde{\boldsymbol{\eta}})|.$$

Any $\tilde{\boldsymbol{\eta}} \in \mathrm{resh}(\tau^j \boldsymbol{\eta})$ on the right hand side will belong to the orbit $[\boldsymbol{\eta}]$ or to some $[\boldsymbol{\eta}'] \overset{v}{\sim} [\boldsymbol{\eta}]$. Since $\tau^j \boldsymbol{\eta}$ and $\tilde{\boldsymbol{\eta}}$ are identical outside the box, it is easy to see that

$$\tilde{C}_v^{-1} \leqslant \frac{\mathcal{N}(\boldsymbol{\eta})^{-1/2}\,|c_j(\boldsymbol{\eta})|}{\mathcal{N}(\tilde{\boldsymbol{\eta}})^{-1/2}\,|c_0(\tilde{\boldsymbol{\eta}})|} \leqslant \tilde{C}_v$$

for some uniform constant $\tilde{C}_v > 0$. Using this estimate and lemma 1, we obtain the following upper bound:

$$M_{[\eta]} \leqslant v!\,\tilde{C}_v\,\mathcal{N}(\boldsymbol{\eta})^{-1} \sum_{r=1}^{d} \sum_{|j-j_r|\leqslant v} |c_j(\boldsymbol{\eta})|^2 \leqslant C'_v\,\mathcal{N}(\boldsymbol{\eta})^{-1} \sum_{r=1}^{d} |c_{j_r}(\boldsymbol{\eta})|^2 = \mathcal{O}_v(\delta)\,.$$

This upper bound holds uniformly for all $[\boldsymbol{\eta}] \in \mathcal{C}_k(z)$, so it also applies to $\|M\|_\infty$ and thus to $r_{\mathrm{sp}}(M)$. Since M is Hermitian, the off-diagonal part in (81) satisfies

$$|d^\dagger M d| = \left| \sum_{[\eta'],[\eta]\in\mathcal{C}_k(z)} \overline{d_{\eta'}}\, M_{[\eta'],[\eta]}\, d_\eta \right| \leqslant r_{\mathrm{sp}}(M)\,\|d\|^2 = \mathcal{O}(\delta).$$

This bound and (82) complete the proof of the first part of theorem 1 dealing with the outer edge of the spectrum.

5.3. Inner edge of the spectrum

The second part of theorem 1 is proved in exactly the same way as the first part, except that the sequences $\boldsymbol{\eta}$ now consist of many (+) and few (−). The Husimi measures of the corresponding eigenstates all converge to a certain measure $\rho_{\min} = \nu_{\min}(\mathrm{d}q) \times \nu_{\mathrm{Can}}(\mathrm{d}p)$, where $\nu_{\min}$ is the self-similar measure defined as follows:

$$\forall v\text{-sequence}\,\boldsymbol{\epsilon}, \qquad \nu_{\min}([\boldsymbol{\epsilon}]) = \prod_{i=1}^{v} |\langle \epsilon_i | f_+\rangle|^2. \tag{85}$$

This measure is supported on the full interval, so that supp $\rho_{\min} = K_+$. One easily checks that $\rho_{\min}$ is conditionally invariant through $\tilde{\mathcal{U}}$ with eigenvalue 1/3. It is a Bernoulli measure of the type considered in [31]. □

Appendix. v-admissible sequences

We fix $v \geqslant 1$ and consider a primitive sequence $\boldsymbol{\eta}$ of length $k \gg v$, which is v-admissible. Our aim is to analyse the structure of this sequence. We will proceed iteratively, from the 'macroscopic scale' ($\sim k$) to the 'microscopic scale' ($\sim v$). At each step, one needs to consider several cases, so that the set of possible structures can be represented by a 'tree' organized into 'levels'. The structure of each admissible $\boldsymbol{\eta}$ will correspond to a 'leaf' of the tree situated at a certain level n (the sequence $\boldsymbol{\eta}$ is then said to have 'rank n'). Each rank-n leaf will be characterized by a sequence of signed integers (64). To fully specify $\boldsymbol{\eta}$ (or rather its orbit $[\boldsymbol{\eta}]$), one further needs to give two 'elementary strings' D_n and R_n. The construction of $\boldsymbol{\eta}$ from these data is explained in section 3.4.1.

We now start to analyse $\boldsymbol{\eta}$. We will present in detail the analysis of the first two levels of $\boldsymbol{\eta}$, and sketch the inductive argument needed to get down to the 'microscopic' level n. Our only assumption is the existence of an admissible pair $j \overset{v,\eta}{\sim} j'$. Up to a global shift of $\boldsymbol{\eta}$, we may assume that $j = 0$ and $0 < j' \leqslant k/2$. We designate $k_1 = j'$ and consider two cases, $k_1 \leqslant v$ and $k_1 > v$.

We recall the notation $\boldsymbol{\eta} \equiv \boldsymbol{\eta}'$ when both sequences belong to the same orbit $[\boldsymbol{\eta}]$; by $|\boldsymbol{\eta}|$ we denote the length of $\boldsymbol{\eta}$. In all decompositions, curly brackets $\{\cdots\}$ will indicate the part of the sequence lying in the v-box.

Appendix A.1. Case $k_1 \leqslant v$: sequences of 'rank 1'

Appendix A.1.1. Structure of the sequence. The assumption $\boldsymbol{\eta} \sim \tau^{-k_1}\boldsymbol{\eta}$ (the fact that the two sequences coincide in the v-bulk), with $0 < k_1 \leqslant v$, is equivalent to the following identity:

$$\eta_{v+1} \dots \eta_k = \eta_{v-k_1+1} \dots \eta_{k-k_1}. \tag{86}$$

(i) If $k_1 \geqslant k - v$, which is possible only when $k \leqslant 2v$, the index sets $\{v + 1, \dots, k\}$ and $\{v - k_1 + 1, \dots, k - k_1\}$ do not overlap. The sequence $\boldsymbol{\eta}$ can be written in terms of two substrings $\boldsymbol{\eta}^1, \boldsymbol{\eta}^f$:

$$\boldsymbol{\eta} = \{\boldsymbol{\eta}^f\,\boldsymbol{\eta}^1\}\,\eta_1^1 \dots \eta_{k-v}^1, \qquad \text{with} \quad |\boldsymbol{\eta}^1| = k_1, \quad |\boldsymbol{\eta}^f| = v - k_1. \tag{87}$$

The two substrings can be chosen independently (as long as they satisfy the condition that $\boldsymbol{\eta}$ is primitive).

(ii) If instead we assume that $k_1 < k - v$, which will be the case in the semiclassical limit, then the two index sets in (86) do overlap. If we call $\boldsymbol{\eta}^1$ the k_1-sequence $\boldsymbol{\eta}^1 = \eta_{v-k_1+1} \dots \eta_v$, then $\boldsymbol{\eta}$ is constructed from a 'free' initial part $\boldsymbol{\eta}^f$ of length $v - k_1$ and the repetition of $\boldsymbol{\eta}^1$:

$$\boldsymbol{\eta} = \{\boldsymbol{\eta}^f\,\boldsymbol{\eta}^1\}\,(\boldsymbol{\eta}^1)^{q_1-1}\,(\eta_1^1 \dots \eta_{l_1}^1) \Longrightarrow \tau^{-l_1}\boldsymbol{\eta} = \tilde{\boldsymbol{\eta}}^f\,(\boldsymbol{\eta}^1)^{q_1}. \tag{88}$$

Here we have applied the Euclidean division $k - v = k_1(q_1 - 1) + l_1$, with $0 \leqslant l_1 < k_1$, and set $\tilde{\boldsymbol{\eta}}^f \stackrel{\text{def}}{=} \eta_1^1 \dots \eta_{l_1}^1 \boldsymbol{\eta}^f$, which has length $< v$. In the nomenclature of section 3.4.1, the sequence (88) has rank 1, with elementary blocks $D_1 = \tilde{\boldsymbol{\eta}}^f$, $R_1 = \boldsymbol{\eta}^1$, and its structure reads ($r_1 = q_1 + 1$).

Remark. The string $\boldsymbol{\eta}^1$ may not be primitive. Assume $\boldsymbol{\eta}^1 = (\tilde{\boldsymbol{\eta}}^1)^m$ for some $m \geqslant 1$, with $\tilde{\boldsymbol{\eta}}^1$ primitive of length $\tilde{k}_1 = k_1/m$. Take $p,\ p'$ maximal such that $\tilde{\boldsymbol{\eta}}^f = (\tilde{\boldsymbol{\eta}}^1)^p\,\boldsymbol{\eta}'\,(\tilde{\boldsymbol{\eta}}^1)^{p'}$, so that

$$\boldsymbol{\eta} \equiv \boldsymbol{\eta}'\,(\tilde{\boldsymbol{\eta}}^1)^{\tilde{q}_1}, \qquad \text{where } \tilde{q}_1 = mq_1 + p + p'. \tag{89}$$

The 'defect' $\boldsymbol{\eta}'$ cannot be empty, otherwise $\boldsymbol{\eta}$ would be periodic.

Appendix A.1.2. Counting the admissible pairs $j \stackrel{v,\eta}{\sim} j'$. We recall that $j \stackrel{v,\eta}{\sim} j'$ means that $\tau^j\boldsymbol{\eta}$ and $\tau^{j'}\boldsymbol{\eta}$ coincide in the v-bulk $\{v + 1, \dots, k\}$. To estimate the number of such pairs, we address the following question: knowing the orbit $[\boldsymbol{\eta}]$ and the v-bulk of $\tau^j\boldsymbol{\eta}$, what do we learn about j?

We separately consider the two cases (87) and (88).

(i) The sequence (87) has length $< 2v$, so the number of pairs is $< 4v^2$.

(ii) Let us consider the sequence (88), or its 'irreducible form' (89). To estimate the number of admissible pairs, we identify a (short) substring of $\boldsymbol{\eta}$ which allows us to identify the position of the defect along $\boldsymbol{\eta}$.

Lemma 2. *The string $\tilde{\boldsymbol{\eta}}^1\,\boldsymbol{\eta}'\,\tilde{\boldsymbol{\eta}}^1$ occurs only once along the sequence $\boldsymbol{\eta} \equiv \boldsymbol{\eta}'\,(\tilde{\boldsymbol{\eta}}^1)^{\tilde{q}_1}$. As a consequence, the string $\boldsymbol{\eta}^1\,\tilde{\boldsymbol{\eta}}^f\,\boldsymbol{\eta}^1$ occurs only once as well.*

Proof. If $\tilde{q}_1 = 2$, the statement is equivalent to the fact that $\boldsymbol{\eta}$ is primitive. When $\tilde{q}_1 \geqslant 3$, a fit of $\tilde{\boldsymbol{\eta}}^1\,\boldsymbol{\eta}'\,\tilde{\boldsymbol{\eta}}^1$ with a different substring of $\boldsymbol{\eta}$ automatically implies that $\tilde{\boldsymbol{\eta}}^1$ is not primitive, which contradicts our assumption. □

As a consequence, if the string $\boldsymbol{\eta}^1\,\tilde{\boldsymbol{\eta}}^f\,\boldsymbol{\eta}^1$ lies in the v-bulk of $\tau^j\boldsymbol{\eta}$, the shift j can be uniquely identified. On the other hand, if $j \stackrel{v,\eta}{\sim} j'$ the string $\boldsymbol{\eta}^1\,\tilde{\boldsymbol{\eta}}^f\,\boldsymbol{\eta}^1$ cannot be fully included in the v-bulk of both partners, but it must intersect the v-box. This string has length $\leqslant 3v$, so both indices $j,\ j'$ must belong to the same interval of length $4v$. Hence, the total number of admissible pairs $j \stackrel{v,\eta}{\sim} j'$ is less than $16v^2$.

Appendix A.2. Case $k_1 > v$

In this subsection we assume that $v < k_1 \leqslant k/2$, then decompose $k - v = (q_1 - 1)k_1 + l_1$, with $0 \leqslant l_1 < k_1$. The assumption $\boldsymbol{\eta} \sim \tau^{-k_1}\boldsymbol{\eta}$ is equivalent to

$$\eta_{v+1} \ldots \eta_k = \eta_{k+v-k_1+1} \ldots \eta_k \eta_1 \ldots \eta_{k-k_1}. \tag{90}$$

This identity implies that $\boldsymbol{\eta}$ is determined by the subsequence $\eta_{v+1} \ldots \eta_{v+k_1}$, which we baptize $\boldsymbol{\eta}^1 = \eta^1_1 \ldots \eta^1_{k_1}$:

$$\boldsymbol{\eta} = \{\eta^1_{k_1-v+1} \ldots \eta^1_{k_1}\}(\boldsymbol{\eta}^1)^{q_1-1}\,(\eta^1_1 \ldots \eta^1_{l_1}). \tag{91}$$

If k_1 and $l_1 + v$ were equal, we would have $k = q_1 k_1$, and the sequence $\boldsymbol{\eta}$ would be k_1-periodic, which is excluded by assumption. Notice that k_1 is *strictly* smaller than $k/2$.

By inserting the above expression for $\boldsymbol{\eta}$ into (90), we obtain a constraint on $\boldsymbol{\eta}^1$:

$$\eta^1_1 \ldots \eta^1_{k_1-v} = \eta^1_{l_1+v+1} \ldots \eta^1_{l_1}, \qquad \text{equivalently } (\boldsymbol{\eta}^1)_i = (\tau^{l_1+v}\boldsymbol{\eta}^1)_i, \quad i = 1, \ldots, k_1 - v. \tag{92}$$

This constraint is similar to (86). To compare the two situations, we also need to know whether $\boldsymbol{\eta}^1$ is primitive.

Lemma 3. *If $k_1 < 2v$ and $\boldsymbol{\eta}^1 = (\tilde{\boldsymbol{\eta}}^1)^m$ with $m > 1$, where $\tilde{\boldsymbol{\eta}}^1$ is primitive of length $\tilde{k}_1 = k_1/m < v$, then we are back to the situation of appendix A.1: $\boldsymbol{\eta}$ is of rank 1, and there exists an admissible pair $j \sim j'$ with $|j - j'| = \tilde{k}_1$.*

If $k_1 \geqslant 2v$, the string $\boldsymbol{\eta}^1$ is necessarily primitive.

Proof. Because $\boldsymbol{\eta}$ is assumed primitive, we do not want $l_1 + v$ to be a period of $\boldsymbol{\eta}^1$. If $\tilde{k}_1 \leqslant k_1 - v$, the constraint (92) and the periodicity of $\boldsymbol{\eta}^1$ imply that this would be the case. In the opposite case $\tilde{k}_1 > k_1 - v$, which can occur only if $k_1 < 2v$, it is possible to realize the constraint (92) for $\boldsymbol{\eta}^1 = (\tilde{\boldsymbol{\eta}}^1)^m$, with $l_1 + v = m'\tilde{k}_1 + k_2$, $0 < k_2 < \tilde{k}_1$: this requires the identity $\tilde{\eta}^1_1 \ldots \tilde{\eta}^1_{k_1-v} = \tilde{\eta}^1_{1+k_2} \ldots \tilde{\eta}^1_{k_1+k_2-v}$. In that case, $\boldsymbol{\eta} \equiv \tilde{\boldsymbol{\eta}} = (\tilde{\boldsymbol{\eta}}^1)^{\tilde{q}_1}\, \tilde{\eta}^1_1 \ldots \tilde{\eta}^1_{k_2}$, which is of the same form as in (89), and forms an admissible pair with $\tau^{-\tilde{k}_1}\tilde{\boldsymbol{\eta}}$. □

In the rest of this section we will assume that $\boldsymbol{\eta}^1$ is primitive, and separately consider the cases $k_1 \gtrless v + l_1$.

Appendix A.2.1. Case $k_1 > v$ with $v + l_1 > k_1$. We may write $v + l_1 = k_1 + k_2$, with, necessarily, $k_2 < v$.

(i) In the case $k_2 \geqslant k_1 - v \stackrel{\text{def}}{=} l_2$ (which can occur only when $k_1 < 2v$), we are in a situation similar to that of appendix A.1, i: the condition (92) does not constrain $\boldsymbol{\eta}^1$ very much, since the index sets $\{1, \ldots, l_2\}$ and $\{1 + k_2, \ldots, l_2 + k_2\}$ do not overlap. In that case,

$$\boldsymbol{\eta}^1 = \boldsymbol{\eta}^2\, \eta^2_1 \ldots \eta^2_{l_2}\, \boldsymbol{\eta}^f = \boldsymbol{\eta}^2\, \tilde{\boldsymbol{\eta}}^f, \qquad \text{with } |\boldsymbol{\eta}^2| = k_2, \quad |\boldsymbol{\eta}^f| = v - k_2, \tag{93}$$

the strings $\boldsymbol{\eta}^2$, $\boldsymbol{\eta}^f$ being independent of one another. We must have $\tilde{\boldsymbol{\eta}}^f \neq \boldsymbol{\eta}^2$, otherwise $\boldsymbol{\eta}$ would be k_2- periodic.

(ii) In the opposite case $k_2 < k_1 - v$, the situation is similar to that in appendix A.1, ii. We divide $k_1 - v = (q_2 - 1)k_2 + l_2$, $0 \leqslant l_2 < k_2$, $q_2 \geqslant 2$. The constraint (92) implies that the sequence $\boldsymbol{\eta}^1$ can be written as

$$\boldsymbol{\eta}^1 = (\boldsymbol{\eta}^2)^{q_2}\, \eta^2_1 \ldots \eta^2_{l_2}\, \boldsymbol{\eta}^f = (\boldsymbol{\eta}^2)^{q_2}\, \tilde{\boldsymbol{\eta}}^f, \qquad |\boldsymbol{\eta}^2| = k_2, \quad |\boldsymbol{\eta}^f| = v - k_2, \tag{94}$$

where the sequences $\boldsymbol{\eta}^2$ and $\boldsymbol{\eta}^f$ are independent. Notice that the sequence (93) has the same form, with $q_2 = 1$. Inserting this expression in (91), we find

$$\boldsymbol{\eta} = \{\eta^2_{l_2+1} \dots \eta^2_{l_2}\, \boldsymbol{\eta}^f\}((\boldsymbol{\eta}^2)^{q_2}\, \tilde{\boldsymbol{\eta}}^f)^{q_1-1}\, (\boldsymbol{\eta}^2)^{q_2}\, \eta^2_1 \dots \eta^2_{l_2}, \tag{95}$$

$$\equiv \tilde{\boldsymbol{\eta}}^f\, (\boldsymbol{\eta}^2)^{q_2+1}\, (\tilde{\boldsymbol{\eta}}^f\, (\boldsymbol{\eta}^2)^{q_2})^{q_1-1}. \tag{96}$$

In the terminology of section 3.4.1, this sequence is of 'rank 2', with the structure $(+q_1, q_2+1)$, and the elementary blocks $D_2 = \tilde{\boldsymbol{\eta}}^f$, $R_2 = \boldsymbol{\eta}^2$.

The sequence $\boldsymbol{\eta}^2$ is not necessarily primitive: it could be of the form $\boldsymbol{\eta}^2 = (\tilde{\boldsymbol{\eta}}^2)^n$ with $\tilde{\boldsymbol{\eta}}^2$ primitive of length $\tilde{k}_2$, and $n > 1$. If we take $p, p' \geqslant 0$ maximal such that $\tilde{\boldsymbol{\eta}}^f = (\tilde{\boldsymbol{\eta}}^2)^p\, \boldsymbol{\eta}'\, (\tilde{\boldsymbol{\eta}}^2)^{p'}$, calling $\tilde{q}_2 = nq_2 + p + p'$, we have

$$\boldsymbol{\eta} \equiv \boldsymbol{\eta}'\, (\tilde{\boldsymbol{\eta}}^2)^{\tilde{q}_2+n}\, (\boldsymbol{\eta}'\, (\tilde{\boldsymbol{\eta}}^2)^{\tilde{q}_2})^{q_1-1}. \tag{97}$$

Notice that $\boldsymbol{\eta}'$ cannot be empty: it is a 'true defect'. The following lemma is proven in a similar way to lemma 2:

Lemma 4. *Assume $\boldsymbol{\eta}^1$ is primitive. Then the string $\tilde{\boldsymbol{\eta}}^2\, \boldsymbol{\eta}'\, \tilde{\boldsymbol{\eta}}^2$ appears exactly q_1 times along $\boldsymbol{\eta}$ of (97). As a consequence, the string $\boldsymbol{\eta}^2\, \tilde{\boldsymbol{\eta}}^f\, \boldsymbol{\eta}^2$ also appears q_1 times along $\boldsymbol{\eta}$.*

Appendix A.2.2. Case $k_1 > v$ with $l_1 + v < k_1$. In this case, the right-hand side in the first equation of (92) reads $\eta^1_{l_1+v+1} \dots \eta^1_{k_1} \eta^1_1 \dots \eta^1_{l_1}$. We define

$$k_2 \stackrel{\text{def}}{=} \min(l_1 + v, k_1 - (l_1 + v)).$$

In the three subcases below we will use the decomposition $k_1 - v = (q_2-1)k_2 + l_2, 0 \leqslant l_2 < k_2$.

Subcase $v + l_1 = k_1 - k_2$ with $0 < k_2 \leqslant v$. In this case we have necessarily $q_1 - 1 \geqslant 2$. Condition (92) implies that

$$\boldsymbol{\eta}^1 = (\boldsymbol{\eta}^2)^{q_2-1}\, \eta^2_1 \dots \eta^2_{l_2}\, \boldsymbol{\eta}^f\, \boldsymbol{\eta}^2 = (\boldsymbol{\eta}^2)^{q_2-1}\, \tilde{\boldsymbol{\eta}}^f\, \boldsymbol{\eta}^2, \qquad |\boldsymbol{\eta}^2| = k_2, \quad |\boldsymbol{\eta}^f| = v - k_2. \tag{98}$$

Notice the similarity to (94). The full sequence reads

$$\boldsymbol{\eta} = \{\boldsymbol{\eta}^f\, \boldsymbol{\eta}^2\}\, ((\boldsymbol{\eta}^2)^{q_2-1}\, \tilde{\boldsymbol{\eta}}^f\, \boldsymbol{\eta}^2)^{q_1-1}\, (\boldsymbol{\eta}^2)^{q_2-2}\, \eta^2_1 \dots \eta^2_{l_2} \tag{99}$$

$$\equiv (\tilde{\boldsymbol{\eta}}^f\, (\boldsymbol{\eta}^2)^{q_2-1})\, (\tilde{\boldsymbol{\eta}}^f\, (\boldsymbol{\eta}^2)^{q_2})^{q_1-1}. \tag{100}$$

This sequence is of rank 2, with the structure $(-q_1, q_2)$ and the elementary blocks $D_2 = \tilde{\boldsymbol{\eta}}^f$, $R_2 = \boldsymbol{\eta}^2$. Lemma 4 also applies here: the string $\boldsymbol{\eta}^2\, \tilde{\boldsymbol{\eta}}^f\, \boldsymbol{\eta}^2$ occurs exactly q_1 times inside $\boldsymbol{\eta}$.

Subcase $v + l_1 = k_2 > v$. From condition (92), we may write

$$\boldsymbol{\eta}^1 = (\boldsymbol{\eta}^2)^{q_2-1}\, (\eta^2_1 \dots \eta^2_{l_2})(\eta^2_{l_2+1} \dots \eta^2_{l_2+v}), \qquad |\boldsymbol{\eta}^2| = k_2. \tag{101}$$

$\boldsymbol{\eta}^2$ satisfies some constraint of the form (92), depending on $v + l_2 \gtrless k_2$.

Subcase $v + l_1 = k_1 - k_2$ with $k_1/2 \geqslant k_2 > v$. Condition (92) imposes that $\boldsymbol{\eta}^1$ can be expressed as

$$\boldsymbol{\eta}^1 = (\boldsymbol{\eta}^2)^{q_2-1}\, (\eta^2_1 \dots \eta^2_{l_2})\, (\eta^2_{k_2-v+1} \dots \eta^2_{k_2}), \qquad |\boldsymbol{\eta}^2| = k_2. \tag{102}$$

$\boldsymbol{\eta}^2$ satisfies some constraint of the form (92), depending on $v + l_2 \gtrless k_2$.

Appendix A.3. Iterating the analysis

In the last two subcases of appendix A.2 ($k_1 > v$ and $k_2 > v$), the level-2 strings $\boldsymbol{\eta}^2$ in (101) or (102) satisfy constraints similar to (90) (for $\boldsymbol{\eta}$) or (92) (for $\boldsymbol{\eta}^1$). The analysis we have performed successively on $\boldsymbol{\eta}$ and $\boldsymbol{\eta}^1$ can be applied to $\boldsymbol{\eta}^2$ and further iterated if necessary. At each step, we find that the sequence $\boldsymbol{\eta}^{j-1} \stackrel{\text{def}}{=} R_{j-1}$ (of length k_{j-1}) is composed of a 'repeated string' $\boldsymbol{\eta}^j \stackrel{\text{def}}{=} R_j$ of length k_j, and a 'defect' D_j, as indicated in (65), (66). This step determines the signed integer $\sigma_j r_j$.

Since $k_j \leqslant k_{j-1}/2$, the lengths $k_1, k_2, \ldots$ decay geometrically with j: for some $n \lesssim \log_2 k$, we end up with a string $\boldsymbol{\eta}^n = R_n$ of length $k_n \leqslant v$, and possibly some extra string $\boldsymbol{\eta}^f$ of length $< v$, which ends the iteration. In general, the level-n defect $\tilde{\boldsymbol{\eta}}^f = D_n$ is obtained by adjoining to $\boldsymbol{\eta}^f$ a strict substring of $\boldsymbol{\eta}^n$. D_n and R_n are the 'elementary strings' of $\boldsymbol{\eta}$. The latter has rank n, structure $(\sigma_1 r_1, \sigma_2 r_2, \ldots, r_n)$, and can be reconstructed from D_n, R_n as explained in section 3.4.1.

By applying lemma 3 at each step, we find that the intermediate sequences $\boldsymbol{\eta}^1, \ldots, \boldsymbol{\eta}^{n-1}$ are primitive. (The blocks D_n and R_n can be nonprimitive, see the remark around (89) and the discussion around (97)).

Appendix A.3.1. Counting admissible pairs $j \stackrel{v,\eta}{\sim} j'$ for admissible sequences of rank n. In this section we prove proposition 2, which estimates the number of admissible pairs $j \stackrel{v,\eta}{\sim} j'$ for an arbitrary v-admissible sequence $\boldsymbol{\eta}$. This counting has already been done for the sequences of rank 1 in appendix A.1.2. Below, the notation $\mathcal{S}_\ell$ will stand for any of the two level-ℓ strings R_ℓ, D_ℓ.

We give ourselves a sequence $\boldsymbol{\eta}$ described by its structure $(\sigma_j r_j)$ and elementary strings D_n, R_n. We want to characterize the admissible pairs $j \stackrel{v,\eta}{\sim} j'$, that is, such that $\tau^j \boldsymbol{\eta}$ and $\tau^{j'} \boldsymbol{\eta}$ coincide outside the v-box. In order to constrain those pairs, we will exhibit proper substrings of $\boldsymbol{\eta}$ which are 'identifiable', or 'recognizable' if they are contained in the v-bulk. For instance, extending lemmas 2 and 4 to sequences of rank n, we see that the string $R_n\, D_n\, R_n$ is recognizable. As a result, a defect D_n can be recognized if its 'neighbourhood' $R_n\, D_n\, R_n$ is contained in the bulk.

The lower level strings $\mathcal{S}_\ell$ can also be recognized if a certain 'neighbourhood' lies in the bulk.

Lemma 5. *For any $\ell \leqslant n-1$ and any level-ℓ string $\mathcal{S}_\ell = R_\ell/D_\ell$ of $\boldsymbol{\eta}$, we consider the following 'neighbourhood' $\hat{\mathcal{S}}_\ell$: from the left end of $\mathcal{S}_\ell$, take $|R_n|$ steps on the left, and $|S_\ell| + |S_{\ell+1}| + \cdots + |S_{n-1}| + 2|R_n| + |D_n|$ steps on the right (here S_i is the short level-i string).*

$\hat{\mathcal{S}}_\ell$ automatically contains $\mathcal{S}_\ell$. If $\hat{\mathcal{S}}_\ell$ is contained in the bulk, then the string $\mathcal{S}_\ell$ it contains can be recognized.

A string which cannot be recognized is said to be 'hidden' by the v-box.

Proof. Consider the level n: to recognize a string $\mathcal{S}_{n-1} = D_n R_n^{r_n(-1)}$, we need to see the defects $R_n\, D_n\, R_n$ adjacent to it, that is, the bulk should contain the string $R_n\, \mathcal{S}_{n-1}\, D_n\, R_n$: from the left end of $\mathcal{S}_{n-1}$, there are $|R_n|$ steps on the left, and $|\mathcal{S}_{n-1}| + |D_n| + |R_n| \leqslant |\mathcal{S}_{n-1}| + 2|R_n| + |D_n|$ steps on the right.

In order to recognize S_{n-2} (respectively L_{n-2}) we need to identify $D_{n-1}\, R_{n-1}^{r_{n-1}-1}\, D_{n-1}$ (respectively $D_{n-1}\, R_{n-1}^{r_{n-1}}$), therefore $R_n\, S_{n-2}\, D_{n-1}\, D_n\, R_n$ (respectively $R_n\, S_{n-2}\, R_{n-1}\, D_n\, R_n$)

must be in the bulk. Whatever the value of σ_{n-1}, the necessary distance on the right is at most $|S_{n-2}| + |S_{n-1}| + 2|R_n| + |D_n|$, while the distance on the left is always $|R_n|$.

The proof for the lower levels proceeds by iteration. □

The identification of a level-ℓ sequence $\mathcal{S}_\ell$ in the bulk of $\tau^j\boldsymbol{\eta}$ implies that the same sequence can be identified at the same site in the bulk of $\tau^{j'}\boldsymbol{\eta}$.

If the level-1 defect D_1 were identifiable, we would have $j = j'$, which contradicts the assumption $j \sim j'$. Thus its neighbourhood $\hat{D}_1$ must intersect the v-box. This provides a first restriction on j, j'.

To identify D_1, it would actually be sufficient to identify the two strings D_2 adjacent to it. To avoid this, the box must intersect one of the two neighbourhoods $\hat{D}_2$ adjacent to D_1.

The lengths $|S_\ell|$ decay geometrically, $|S_{\ell+1}| < |S_\ell|/2$, so that $|\hat{D}_2|$ is bounded from above by $|S_2| + 2|S_3| + 4v$. On the other hand, $|D_2R_2| = 2|S_2| + |R_3| \geqslant 2|S_2| + |S_3|$. Let us assume that $|S_2| > 20v$. We then draw

$$|D_2R_2| - |\hat{D}_2| \geqslant |S_2| - |S_3| - 4v > |S_2|/2 - 4v > 6v.$$

As a result, the box can intersect at most a single one of the r_1 neighbourhoods $\hat{D}_2$, the other $r_1 - 1$ strings $\hat{D}_2$ sitting in the bulks of $\tau^j\boldsymbol{\eta}$ and $\tau^{j'}\boldsymbol{\eta}$. This implies that

$$j' = j + k_1 \quad \text{if the hidden } D_2 \text{ is on the left of } D_1,$$

$$\text{respectively } j' = j - k_1 \quad \text{if the hidden } D_2 \text{ is on the right of } D_1.$$

In the two cases, the two partners correspond to an exchange (a 'flip') of two level-1 strings:

$$R_1D_1 \to D_1R_1, \qquad \text{respectively } D_1R_1 \to R_1D_1.$$

Let us consider the first alternative ($j' = j + k_1$), and zoom on the string $\hat{D}_2$ which intersects the box. Actually, to identify the D_2 it contains, it would be sufficient to identify both level-3 strings D_3 adjacent to it. The box must thus intersect at least one of the neighbourhoods $\hat{D}_3$. Once more, if $|S_3| > 20v$, only one of these neighbourhoods can be hidden. The choice of the hidden D_3 depends on σ_1. Assume for instance $\sigma_1 = -$, so that the defect $D_1 = L_1 = D_2\,R_2^{r_2}$. The flip $R_1D_1 \to D_1R_1$ then reads

$$D_2\,R_2^{r_2-1}\,D_2\,R_2\,R_2^{r_2-1} \to D_2\,R_2^{r_2-1}\,R_2\,D_2\,R_2^{r_2-1},$$

which involves the level-2 flip $D_2\,R_2 \to R_2\,D_2$. This shows that it is the string D_3 situated at the *right* of D_2, that is the one at the junction $D_2\,R_2$, which should be hidden. Iterating to higher levels, we see that, as long as $k_\ell \gg v$, the exchange $\tau^j\boldsymbol{\eta} \to \tau^{j+k_1}\boldsymbol{\eta}$ involves either the flip $D_\ell\,R_\ell \to R_\ell\,D_\ell$ or the opposite one, and the string $D_{\ell+1}$ at the junction must be hidden: the box must intersect the corresponding neighbourhood $\hat{D}_{\ell+1}$. The iteration stops when $|S_\ell| \leqslant 20v$. At this stage, the intersection of the box with D_ℓ implies that j must be contained in some interval of length $\leqslant 42v$ around the corresponding D_ℓ. Since its partner j' is uniquely fixed by j, this proves the estimate in proposition 2. □

Appendix A.4. Variations of the coefficients $c_{jm}(\boldsymbol{\eta})$ for admissible sequences

In this section we will prove proposition 3, that is we show that, for a sequence $\boldsymbol{\eta}$ admitting partners $j \overset{v,\boldsymbol{\eta}}{\sim} j'$, all coefficients $|c_{jm}|$ are approximately of the same size.

Appendix A.4.1. An alternative description of level-ℓ strings. We will represent rank-n admissible sequences $\boldsymbol{\eta}$ in a slightly different manner than in section 3.4.1. Instead of characterizing, at each level ℓ, the strings D_ℓ and R_ℓ by their lengths ('long' versus 'short'), we will rather distinguish them by the relative number of elementary strings R_n, D_n they are composed of. That is, we will label differently the branches and leaves of the tree representing the possible admissible structures.

By convention, let us call 'positive' (respectively 'negative') the elementary strings:

$$P_n \stackrel{\text{def}}{=} D_n = \tilde{\boldsymbol{\eta}}^f, \qquad N_n \stackrel{\text{def}}{=} R_n = \boldsymbol{\eta}^n.$$

The two level-$(n-1)$ strings are now called as follows:

$$N_{n-1} = P_n\, N_n^{r_n}, \qquad P_{n-1} = P_n\, N_n^{r_n-1}. \tag{103}$$

Obviously, N_{n-1} is the string containing more repetitions of N_n.

The construction of the lower levels proceeds by an iteration which is different but similar to the one in (65) and (66). Starting from strings N_ℓ, P_ℓ at level $\ell < n$, we define a 'positive' and a 'negative' string at level $\ell - 1$ by the following rule: $P_{\ell-1}$ is the string with the highest number of P_ℓ or the lowest number of N_ℓ. The explicit form of $N_{\ell-1}$ and $P_{\ell-1}$ depends on a signed integer $\varsigma_\ell r_\ell$, where r_ℓ is the same as in (64):

$$\begin{pmatrix} N_{\ell-1} \\ P_{\ell-1} \end{pmatrix} = \begin{pmatrix} N_\ell^{r_\ell}\, P_\ell \\ N_\ell^{r_\ell-1}\, P_\ell \end{pmatrix} (\varsigma_\ell = +) \qquad \text{versus}$$
$$\begin{pmatrix} N_{\ell-1} \\ P_{\ell-1} \end{pmatrix} = \begin{pmatrix} N_\ell\, P_\ell^{r_\ell-1} \\ N_\ell\, P_\ell^{r_\ell} \end{pmatrix} (\varsigma_\ell = -). \tag{104}$$

Except at level n, we always place the N_ℓ to the left of the P_ℓ, so the above sequences are generally equal to D_ℓ or R_ℓ only up to appropriate shifts. The sign $\varsigma_\ell \in \{\pm\}$ indicates whether the defect D_ℓ is (up to a shift) equal to P_ℓ or N_ℓ. The string N_ℓ is a shift of either L_ℓ or S_ℓ, the choice depending on the signs $\{\sigma_{n-1}, \ldots, \sigma_{\ell+1}\}$, or equivalently $\{\varsigma_{n-1}, \ldots, \varsigma_{\ell+1}\}$.

To be more synthetic, we call $P_\ell = \mathcal{S}_\ell^+$ and $N_\ell = \mathcal{S}_\ell^-$. The iteration (104) means that the sequence $\mathcal{S}_j^{\varsigma_j}$ is the level-j defect, while $\mathcal{S}_j^{-\varsigma_j}$ is repeated r_j or $r_j - 1$ times in $\mathcal{S}_{j-1}^{\pm}$. The first integer ($-r_1$ versus $+r_1$) corresponds to the global (lowest-level) structure of $\boldsymbol{\eta}$: for a certain shift $\tilde{\boldsymbol{\eta}} \equiv \boldsymbol{\eta}$ one has

$$\tilde{\boldsymbol{\eta}} = N_1^{r_1-1}\, P_1\ (\varsigma_1 = +) \quad \text{versus} \quad \tilde{\boldsymbol{\eta}} = N_1\, P_1^{r_1-1}\ (\varsigma_1 = -),$$
$$\text{in short} \quad \tilde{\boldsymbol{\eta}} \equiv (\mathcal{S}_1^{-\varsigma_1})^{r_1-1}\, (\mathcal{S}_1^{\varsigma_1}). \tag{105}$$

We notice that $\boldsymbol{\eta}$ contains more sequences $N_n = R_n$ than $P_n = D_n$.

Appendix A.4.2. Variations of the $|c_{jm}(\boldsymbol{\eta})|$. Let $\boldsymbol{\eta}$ be the sequence described above, with relative degree $\delta = d/k$. We first consider coefficients $|c_{jm}(\tilde{\boldsymbol{\eta}})|$ associated with the particular shift $\tilde{\boldsymbol{\eta}}$ of $\boldsymbol{\eta}$ described in (105). The logarithms of the coefficients $|c_{jm}(\tilde{\boldsymbol{\eta}})|$ (as in (74)) can be expressed in terms of a single (δ-dependent) function

$$B : \bigsqcup_{n\geqslant 0} \{+,-\}^n \longrightarrow \mathbb{R}$$

$$\boldsymbol{\alpha} = \alpha_1 \cdots \alpha_n \longmapsto B(\boldsymbol{\alpha}) = \sum_{s=1}^{n} \log \left| \frac{\lambda_{\alpha_s}}{\lambda^\delta} \right|,$$

where we recall that $\lambda_- = 1$, $\lambda_+ = \lambda = i/\sqrt{3}$. We then have $\log|c_{jm}(\tilde{\boldsymbol{\eta}})| = B(\tilde{\eta}_1 \cdots \tilde{\eta}_j)$. As noticed in section 5.1, these coefficients form a discrete path made of a succession of 'ups' $\delta\Lambda$ and 'downs' $(\delta - 1)\Lambda$, with $\Lambda = -\log|\lambda|$.

For any n-string $\boldsymbol{\alpha}$ we have the obvious bound

$$|B(\alpha_1 \cdots \alpha_n)| \leqslant n\,\Lambda. \tag{106}$$

In the previous paragraph we have decomposed $\tilde{\boldsymbol{\eta}}$ into substrings, starting at the highest level with the string P_n which initiates $\tilde{\boldsymbol{\eta}}$, and N_n which follows it. We renormalize the function B by defining

$$b(\bullet) \stackrel{\text{def}}{=} \frac{B(\bullet)}{B(P_n)}.$$

Equivalently, this function is defined as the unique function on $\bigsqcup_{n\geqslant 0}\{+,-\}^n$, such that

$$b(P_n) = 1, \qquad b(\tilde{\boldsymbol{\eta}}) = 0 \qquad \text{and} \qquad b(\boldsymbol{\alpha}\boldsymbol{\beta}) = b(\boldsymbol{\alpha}) + b(\boldsymbol{\beta}).$$

Since $|P_n| \leqslant v$, the bound (106) shows that $|B(P_n)| \leqslant \Lambda v$. To prove proposition 3 we will control the variations of the sequence

$$\{b(\tilde{\boldsymbol{\eta}}_1 \cdots \tilde{\boldsymbol{\eta}}_n),\ 0 \leqslant n \leqslant k\}. \tag{107}$$

Since $\tilde{\boldsymbol{\eta}}$ contains more strings N_n than P_n and $b(\tilde{\boldsymbol{\eta}}) = 0$, we have

$$-1 < b(N_n) < 0 < b(P_n) = 1.$$

Inspecting the alternative (104), we see that at each level $1 \leqslant \ell < n$, we have again

$$-1 < b(N_\ell) < 0 < b(P_\ell) < 1. \tag{108}$$

This property reflects the name 'positive' versus 'negative'. We can further constrain the values $b(N_\ell)$, $b(P_\ell)$.

Let us call $\#_\ell^\pm$ the number of level-ℓ strings $\mathcal{S}_\ell^\pm$ contained in the rank-n sequence $\tilde{\boldsymbol{\eta}}$. The following lemma relates this cardinal to the values of $b(\mathcal{S}_\ell^\pm)$.

Lemma 6. *There exists a real number $c > 0$ such that, at each level $1 \leqslant \ell \leqslant n$, one has*

$$b(N_\ell) = -c\,\#_\ell^+, \qquad b(P_\ell) = c\,\#_\ell^- \qquad \text{or concisely} \qquad b(\mathcal{S}_\ell^\pm) = \pm c\,\#_\ell^\mp. \tag{109}$$

The normalization condition $b(P_n) = 1$ implies that $c = (\#_n^-)^{-1}$.

Proof. We reason by recurrence on increasing ℓ. From (105) we have at level $\ell = 1$:

$$0 = b(\tilde{\boldsymbol{\eta}}) = (r_1 - 1)\,b(\mathcal{S}_1^{-\varsigma_1}) + b(\mathcal{S}_1^{\varsigma_1}) \qquad \text{and} \qquad \#_1^{-\varsigma_1} = r_1 - 1, \quad \#_1^{\varsigma_1} = 1.$$

This means that there exists a real number c such that

$$b(\mathcal{S}_1^{\varsigma_1}) = \varsigma_1\,c\,(r_1 - 1) = \varsigma_1\,c\,\#_1^{-\varsigma_1}, \qquad b(\mathcal{S}_1^{-\varsigma_1}) = -\varsigma_1\,c = -\varsigma_1\,c\,\#_1^{\varsigma_1}.$$

From (108) we must have $c > 0$. Let us now assume the property (109) for some $\ell - 1 \geqslant 1$, and first treat the case $\varsigma_\ell = +$, so that the numbers of sequences of level ℓ are

$$\#_\ell^+ = \#_{\ell-1}^+ + \#_{\ell-1}^-$$
$$\#_\ell^- = (r_\ell - 1)\#_{\ell-1}^+ + r_\ell\,\#_{\ell-1}^-.$$

At the same time, we easily extract the coefficients $b(\mathcal{S}_\ell^\pm)$:

$$\begin{cases} r_\ell\,b(N_\ell) + b(P_\ell) = -c\,\#_{\ell-1}^+ \\ (r_\ell - 1)\,b(N_\ell) + b(P_\ell) = c\,\#_{\ell-1}^- \end{cases} \iff \begin{cases} b(N_\ell) = -c\,(\#_{\ell-1}^+ + \#_{\ell-1}^-) = -c\,\#_\ell^+ \\ b(P_\ell) = c\,((r_\ell - 1)\#_{\ell-1}^+ + r_\ell\,\#_{\ell-1}^-) = c\,\#_\ell^-. \end{cases}$$

This proves the property at level ℓ. The case $\varsigma_\ell = -$ is similar. □

Lemma 7. *Take $\tilde{\eta}$ admissible of rank n. Then, the values of b on the defects $\mathcal{S}_\ell^{\varsigma_\ell}$ satisfy*

$$\mathrm{Sum}(\tilde{\eta}) \stackrel{\mathrm{def}}{=} \sum_{\ell=1}^{n-1} |b(\mathcal{S}_\ell^{\varsigma_\ell})| = \sum_{\ell=1}^{n-1} \varsigma_\ell\, b(\mathcal{S}_\ell^{\varsigma_\ell}) < 1\,.$$

Proof. From (109), the above sum reads $\mathrm{Sum}(\tilde{\eta}) = \frac{1}{\#_n^-} \sum_{\ell=1}^{n-1} \#_\ell^{-\varsigma_\ell}$. On the other hand, if we call $\#_\ell = \#_\ell^+ + \#_\ell^-$ the total number of level-ℓ strings, we check by recurrence that

$$\forall \ell \leqslant n-1, \qquad \#_\ell = 1 + \sum_{l=1}^{\ell} \#_l^{-\varsigma_l}.$$

Indeed, we already have $\#_1 = \#_1^{\varsigma_1} + \#_1^{-\varsigma_1} = 1 + (r_1 - 1)$. Assuming the above equality at level $\ell - 1$, the number of ℓ-defects $\#_\ell^{\varsigma_\ell}$ is equal to the number $\#_{\ell-1}$ of level-$(\ell-1)$ strings (one defect for each string), so that

$$\#_{\ell-1} + \#_\ell^{-\varsigma_\ell} = \#_\ell^{\varsigma_\ell} + \#_\ell^{-\varsigma_\ell} = \#_\ell.$$

This proves the recurrence. Thus, taking $\ell = n-1$ we get

$$\mathrm{Sum}(\tilde{\eta}) = \frac{\#_{n-1} - 1}{\#_n^-} = \frac{\#_n^+ - 1}{\#_n^-}.$$

Finally, $\#_n^+ < \#_n^-$ (these are respectively the numbers of strings P_n and N_n). □

We can now finish the proof of proposition 3. For any level $1 \leqslant \ell \leqslant n$, we call b^ℓ the 'sampling' of the sequence (107) obtained by keeping only the successions of blocks of level ℓ, starting from $b(\emptyset) = 0$, $b(N_\ell)$, and finally reaching $b(\tilde{\eta}) = 0$. The sequence $b^{\ell+1}$ is thus a 'refinement' of b^ℓ.

We first describe the level $\ell = 1$. If $\varsigma_1 = -$, we have $b^1 \stackrel{\mathrm{def}}{=} (0, b(N_1), b(N_1 P_1), \ldots, b(N_1 P_1^{r_1 - 1}) = 0)$. Its smallest value $b(N_1)$ is reached after a 'steep drop', then the sequence increases at a slower rate to finally reach 0 again. In the opposite case $\varsigma_1 = +$, the sequence $b^1 = (0, b(N_1), b(N_1^2), \ldots, 0)$ first slowly decays until it reaches $b(N_1^{r_1-1})$, then it makes its largest (positive) variation $b(P_1)$ to jump back to 0. Its smallest value is $b(N_1^{r_1-1}) = -b(P_1)$. In both cases, the minimal value of b^1 is $-|b(\mathcal{S}_1^{\varsigma_1})|$.

Let us now study the variations of b at the level $2 < n$. First assume $\varsigma_1 = \varsigma_2 = -$, so the sequence $b^2 = (0, b(N_2), b(N_2 P_2), \ldots, b(N_1), \ldots, 0)$. It first has a big negative jump $b(N_2)$, followed by $r_2 - 1$ small positive jumps to reach $b(N_1) < 0$, the smallest value of b^1. Then starts the level-2 string composing $P_1 = N_2 P_2^{r_2}$. From $b(N_1)$ we have a steep negative jump to $b(N_1 N_2)$, then r_2 smaller positive jumps to reach $b(N_1 P_1) > b(N_1)$. The following negative jumps in b^2 will never bring it as low as the value $b(N_1 N_2) = b(N_1) + b(N_2)$, which is hence its smallest value. On the other hand, all elements of b^2 (but the first and last) are negative.

If $\varsigma_1 = -$, $\varsigma_2 = +$, we first have r_2 small negative jumps to reach $b(N_2^{r_2})$, followed by a larger positive jump of $b(P_2)$ to reach $b(N_1) < 0$. Then, we have again $r_2 - 1$ negative jumps to $b(N_1 N_2^{r_2-1})$, and a following positive jump of $b(P_2)$ to get $b(N_1 P_1) > b(N_1)$. The following values will consist of adding $b(P_1)$ to already existing values, so they cannot get smaller. The smallest value of b^2 for this case is thus $b(N_2^{r_2}) = b(N_1) - b(P_2)$.

The case $\varsigma_1 = +$ is equivalent to the 'time reversal' of the sequences b^2 described above. In all cases, the minimum of b^2 occurs one step after or before the minimum of b^1, and its value is given by

$$\min b^2 = \min b^1 - |b(\mathcal{S}_2^{\varsigma_2})| = -|b(\mathcal{S}_1^{\varsigma_1})| - |b(\mathcal{S}_2^{\varsigma_2})|.$$

The reasoning can be pursued to find that at any level $\ell \leqslant n-1$, the minimum of the sequence b^ℓ is given by $\min b^\ell = -\sum_{l=1}^{\ell} |b(\mathcal{S}_l^{\varsigma_l})|$, and that b^ℓ takes negative values except at its start and end. At level $\ell = n-1$, we thus get $\min b^{n-1} = -\mathrm{Sum}(\tilde{\boldsymbol{\eta}})$. Once we know $b^{n-1} = (0, b(N_{n-1}), \ldots)$, the sequence b^n starts with $b(P_n) = 1$, followed by $r_n - 1$ decays until it reaches $b(N_{n-1}) < 0$. Since all values of b^{n-1} are negative, we have $b_i^{n-1} + b(P_n) \leqslant 1$ for any index i. On the other hand, the value of b^n never becomes smaller than $\min b^{n-1}$. As a result, using lemma 7 we find that all the elements of b^n are bounded by

$$-1 < -\mathrm{Sum}(\tilde{\boldsymbol{\eta}}) \leqslant b_i^n \leqslant 1, \qquad 0 \leqslant i \leqslant \#_n.$$

By multiplying these inequalities by $B(P_n)$, we find that the components of the rescaled sequence B^n satisfy $|B_i^n| \leqslant \Lambda v$. Finally, each string $\tilde{\eta}_1 \ldots \tilde{\eta}_j$ is at most at 'distance' $[v/2]$ from some string at level n, so using (106) we get the bound $|B(\tilde{\boldsymbol{\eta}}_1 \cdots \tilde{\boldsymbol{\eta}}_i)| = \log |c_{im}(\tilde{\boldsymbol{\eta}})| \leqslant 3\Lambda v/2$ for any $0 \leqslant i \leqslant k$.

Finally, the cocycle property $c_{jm}(\tau^\ell \tilde{\boldsymbol{\eta}}) = \frac{c_{(j+\ell)m}(\tilde{\boldsymbol{\eta}})}{c_{\ell m}(\tilde{\boldsymbol{\eta}})}$ proves proposition 3 for an arbitrary shift $\boldsymbol{\eta}$ of $\tilde{\boldsymbol{\eta}}$. □

Acknowledgments

This work was supported by EPSRC. S N was partially supported by the Agence Nationale de la Recherche, under the grant ANR-05-JCJC-0107-01. He is grateful to Jens Marklof for organizing a session at the School of Mathematics in Bristol, during which this collaboration was initiated.

References

[1] Anantharaman N and Nonnenmacher S 2007 Entropy of semiclassical measures of the Walsh-quantized baker's map *Ann. Henri Poincaré* **8** 37
[2] Balazs N L and Voros A 1989 The quantized Baker's transformation *Ann. Phys. (NY)* **190** 1
[3] Berkolaiko G, Keating J P and Smilansky U 2007 Quantum ergodicity for graphs related to interval maps *Commun. Math. Phys.* **273** 137
[4] Berkolaiko G, Keating J P and Winn B 2003 Intermediate wave function statistics *Phys. Rev. Lett.* **91** 134103
[5] Berkolaiko G, Keating J P and Winn B 2004 No quantum ergodicity for star graphs *Commun. Math. Phys.* **250** 259
[6] Berry M V 1977 Regular and irregular semiclassical wavefunctions *J. Phys.* A **10** 2083
[7] Bouzouina A and De Bièvre S 1996 Equipartition of the eigenfunctions of quantized ergodic maps on the torus *Commun. Math. Phys.* **178** 83
[8] Casati G, Maspero G and Shepelyansky D L 1999 Quantum fractal eigenstates *Physica* D **131** 311
[9] Chang C-H, Krüger T, Schubert R and Troubetzkoy S E 2007 Quantizations of piecewise affine maps on the torus and their quantum limits arXiv:0704.2692
[10] Chernov N and Markarian R 1997 Ergodic properties of Anosov maps with rectangular holes *Bol. Soc. Bras. Mat.* **28** 271
[11] Colin de Verdière Y 1985 Ergodicité et fonctions propres du laplacien *Commun. Math. Phys.* **102** 497
[12] Degli Esposti M, Nonnenmacher S and Winn B 2006 Quantum variance and ergodicity for the baker's map *Commun. Math. Phys.* **263** 325
[13] Degli Esposti M and Graffi S (ed) 2003 *The Mathematical Aspects of Quantum Maps* (*Lecture Notes in Physics*) (Berlin: Springer)
[14] Demers M F and Young L S 2006 Escape rates and conditionally invariant measures *Nonlinearity* **19** 377
[15] Ermann L and Saraceno M 2006 Generalized quantum baker maps as perturbations of a simple kernel *Phys. Rev.* E **74** 046205
[16] Faure F, Nonnenmacher S and De Bièvre S 2003 Scarred eigenstates for quantum cat maps of minimal periods *Commun. Math. Phys.* **239** 449
[17] Guillopé L, Lin K and Zworski M 2004 The Selberg zeta function for convex co-compact Schottky groups *Commun. Math. Phys.* **245** 149

[18] Hannay J H and Berry M V 1980 Quantization of linear maps on a torus - fresnel diffraction by a periodic grating *Physica* D **1** 267

[19] Hannay J H, Keating J P and Ozorio de Almeida A M 1994 Optical realization of the baker's transformation *Nonlinearity* **7** 1327

[20] Helffer B, Martinez A and Robert D 1987 Ergodicité et limite semi-classique *Commun. Math. Phys.* **109** 313

[21] Keating J P 1991 The cat maps: quantum mechanics and classical motion *Nonlinearity* **4** 309

[22] Keating J P, Mezzadri F and Robbins J M 1999 Quantum boundary conditions for torus maps *Nonlinearity* **12** 579

[23] Keating J P, Novaes M, Prado S and Sieber M 2006 Semiclassical structure of chaotic resonance eigenfunctions *Phys. Rev. Lett.* **97** 150406

[24] Kurlberg P and Rudnick Z 2000 Hecke theory and equidistribution for the quantization of linear maps of the torus *Duke Math. J.* **103** 47

[25] Kurlberg P, Rosenzweig L and Rudnick Z 2007 Matrix elements for the quantum cat map: fluctuations in short windows *Nonlinearity* **20** 2289

[26] Kurlberg P and Rudnick Z 2001 On quantum ergodicity for linear maps of the torus *Commun. Math. Phys.* **222** 201

[27] Lin K K and Zworski M 2002 Quantum resonances in chaotic scattering *Chem. Phys. Lett.* **355** 201

[28] Lindenstrauss E 2006 Invariant measures and arithmetic quantum unique ergodicity *Ann. Math.* **163** 165

[29] Lu W, Sridhar S and Zworski M 2003 Fractal Weyl law for chaotic open systems *Phys. Rev. Lett.* **91** 154101

[30] Marklof J and Rudnick Z 2003 Quantum unique ergodicity for parabolic maps *Geom. Funct. Anal.* **10** 1554

[31] Nonnenmacher S and Rubin M 2007 Resonant eigenstates for a quantized chaotic system *Nonlinearity* **20** 1387

[32] Nonnenmacher S and Zworski M 2005 Fractal Weyl laws in discrete models of chaotic scattering *J. Phys.* A **38** 10683

[33] Nonnenmacher S and Zworski M 2007 Distribution of resonances for open quantum maps *Commun. Math. Phys.* **269** 311

[34] Rosenzweig L 2006 Quantum unique ergodicity for maps on the torus *Ann. Henri Poincaré* **7** 447

[35] Rudnick Z and Sarnak P 1994 The behaviour of eigenstates of arithmetic hyperbolic manifolds *Commun. Math. Phys.* **161** 195

[36] Saraceno M 1990 Classical structures in the quantized baker transformation *Ann. Phys. (NY)* **199** 37

[37] Saraceno M and Vallejos R O 1996 The quantized D-transformation *Chaos* **6** 193

[38] Schack R and Caves C M 2000 Shifts on a finite qubit string: a class of quantum baker's maps *Appl. Algebra Eng. Commun. Comput.* **10** 305

[39] Schomerus H and Tworzydlo J 2004 Quantum-to-classical crossover of quasibound states in open quantum systems *Phys. Rev. Lett.* **93** 154102

[40] Shnirelman A I 1974 Ergodic properties of eigenfunctions *Usp. Mat. Nauk.* **29** 181

[41] Sjöstrand J and Zworski M 2007 Fractal upper bounds on the density of semiclassical resonances *Duke Math. J.* **137** 381

[42] Thiele C 1995 Time-frequency analysis in the discrete phase plane *PhD Thesis* Yale university

[43] Voros A 1979 Semi-classical ergodicity of quantum eigenstates in the Wigner representation *Stochastic Behavior in Classical and Quantum Hamiltonian Systems* ed G Casati and J Ford (Berlin: Springer) p 326

[44] Zelditch S 1987 Uniform distribution of eigenfunctions on compact hyperbolic surfaces *J. Phys.* A **20** 2415

[45] Zelditch S 2006 *Quantum Ergodicity and Mixing* (*Encyclopedia of Mathematical Physics*) vol 4 ed J-P Françoise *et al* (Amsterdam: Elsevier) pp 183–96